3

Fluorescence Microscopy

Jurek W. Dobrucki[1] *and Ulrich Kubitscheck*[2]

[1] *Jagiellonian University, Faculty of Biochemistry, Biophysics and Biotechnology, Department of Cell Biophysics of Cell Biophysics, ul Gronostajowa 7, Krakow 30-387, Poland*
[2] *Rheinische Friedrich-Wilhelms-Universität Bonn, Institut für Physikalische & Theoretische Chemie, Wegelerstr. 12, Bonn 53115, Germany*

3.1 Contrast in Optical Microscopy

The human eye requires contrast to perceive details of objects. Several ingenious methods of improving the contrast of microscopy images have been designed, and each of them opened new applications of optical microscopy in biology. The simplest and very effective contrasting method is "dark field." It exploits the scattering of light on small particles that differ from their environment in refractive index – the phenomenon known in physics as the *Tyndall effect*. Color staining of a preparation can provide even more information. A fixed and largely featureless preparation of tissue may reveal a lot of its structure if stained with a proper dye – a substance that recognizes specifically some tissue or cellular structure and absorbs light of a specific wavelength. This absorption results in a perception of color. The pioneers of histochemical staining of biological samples were Camillo Golgi, an Italian physician, and Santiago Ramon y Cajal, a Spanish pathologist. They received the 1906 Nobel Prize for Physiology or Medicine. A revolutionary step in the development of optical microscopy was the introduction of phase contrast proposed by the Dutch scientist Frits Zernike. This was such an important discovery that Zernike was awarded the 1953 Nobel Prize in Physics. The ability to observe fine subcellular details in an unstained specimen opened new avenues of research in biology. Light that passes through a specimen may change polarization characteristics. This is a phenomenon exploited in polarization microscopy, a technique that has also found numerous applications in materials science. The next important step in creating contrast in optical microscopy came with an invention of differential interference contrast by Jerzy (Georges) Nomarski, a Polish scientist who had to leave Poland after World War II and worked in France. In his technique, the light incident on the sample is split into two closely spaced beams of polarized light, where the planes of polarization are perpendicular to each other. Interference of the two beams after they have passed through the specimen results in excellent contrast, which creates an impression of three-dimensionality of the object.

Fluorescence Microscopy: From Principles to Biological Applications, Second Edition.
Edited by Ulrich Kubitscheck.

However, by far the most popular contrasting technique now is fluorescence. It requires the use of so-called fluorochromes or fluorophores, which absorb light in a specific wavelength range and re-emit photons of lower energy, that is, shifted to a longer wavelength. Today, a very large number of different dyes with absorption from the ultraviolet (UV) to the near-infrared (NIR) region are available, and more fluorophores with new properties are still being developed (see Chapter 4). The principal advantages of this approach are very high contrast, sensitivity, specificity, and selectivity. The first dyes used in fluorescence microscopy were not made specifically for research, but were taken from a collection of stains used for coloring fabrics. The use of fluorescently stained antibodies and the introduction of a variety of fluorescent heterocyclic probes synthesized for specific biological applications brought about an unprecedented growth in biological applications of fluorescence microscopy. Introduction of fluorescent proteins sparked a new revolution in microscopy, contributed to the development of a plethora of new microscopy techniques, and enabled the recent enormous growth of optical microscopy and new developments in cell biology. A Japanese scientist, Osamu Shimomura, and two American scientists, Martin Chalfie and Robert Y. Tsien, were awarded the Nobel Prize for Chemistry in 2008 for "the discovery and development of the green fluorescent protein, 'GFP', in biological research." The next milestone in the unstoppable progress of modern fluorescence microscopy was reached when the super-resolution (or "sub-diffraction" resolution) imaging techniques became available. Their potential and importance in biological studies were soon recognized, and a climax of these developments was a 2014 Nobel Prize in Chemistry awarded to Eric Betzig, Stefan W. Hell, and William E. Moerner for "the development of super-resolved fluorescence microscopy."

The use of fluorophores requires several critical modifications in the illumination and imaging beam paths of an optical microscope. Fluorescence excitation requires specific light sources, and their emission is often recorded with advanced electronic light detection devices. However, fluorescence exhibits important limitations: fluorescent dyes have a limited stability, that is, they photobleach, and may induce phototoxic effects. This requires special precautions to be taken. We discuss, first, the physical basis of fluorescence, and then present the major technical and methodological questions involved in this chapter.

3.2 Physical Foundations of Fluorescence

3.2.1 What is Fluorescence?

Fluorophores are molecules or nanocrystals with a special property. They absorb photons of a certain energy and emit photons of a lower energy. Considering the electromagnetic spectrum, this means that the color of the emitted light is red-shifted with respect to the absorbed light. As explained previously, this effect can elegantly be used to generate a superb contrast in microscopy. So, how does this effect work in detail? We focus here on fluorescent molecules because these are by far the most often used fluorophores in microscopy.

The absorbing fluorescent molecule comprises a set of atoms that share a number of delocalized electrons in molecular orbitals with specific spatial charge distributions. We may say that the negatively charged electrons represent the *glue* that keeps the positively charged atomic nuclei close together to stabilize the molecule. The electronic ground state is typically a singlet state, designated as S_0. The spins of both electrons in this electronic orbital are antiparallel to each other. Upon absorption of light, that is, a photon, one of the electrons is lifted into another orbital, typically into the first excited singlet state, S_1. By the excitation from the ground state the spin of the excited electron is not flipped, therefore the spin of the excited electron is still antiparallel to that of the single electron left behind in its original molecular orbital. Energy conservation requires that the energy of the absorbed photon equals the energy difference between the ground state and the excited state. In the excited state, the overall charge distribution of the electrons around the atomic nuclei is altered compared to the ground state. A key point is that the electrons change their spatial distribution almost instantaneously – within femtoseconds – whereas the much heavier atomic nuclei move more slowly and take significantly longer – picoseconds – to relax to the new charge distribution of the electrons. The excited electron is relocated into a *higher* orbital with a greater distance from the nuclei than before, which results in a relaxation of the molecular structure that usually initiates a vibration of the complete molecule about the new equilibrium positions of the atoms. However, the vibrational energy rapidly dissipates upon collisions with the surrounding solvent molecules as heat, and the molecule decays into the vibrational ground state of the electronically excited state S_1 (Figure 3.1). However, since

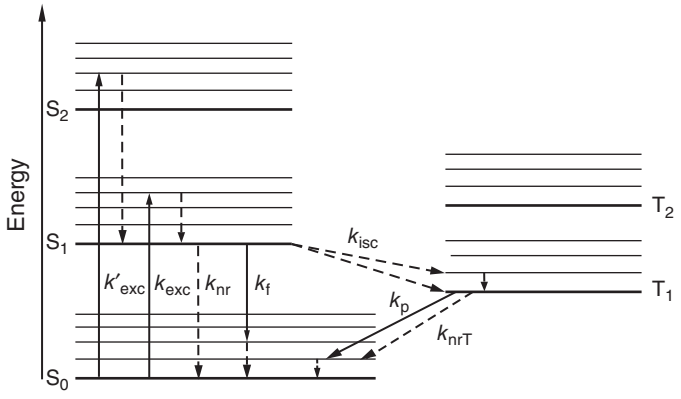

Figure 3.1 Simplified Jablonski diagram or molecular term scheme. Radiative and nonradiative transitions are indicated by full and dashed lines, respectively. "Energy" refers to the total potential and kinetic energy of electrons and atomic nuclei. For a discussion of the scheme, see text. Fluorescence studies on single molecules have shown that sometimes there are further nonfluorescent molecular configurations with lifetimes in the range of milliseconds to seconds. After leaving these long-lived states, the molecules may return to the normal fluorescence process. This effect is called "reversible" photobleaching, and, if occurring repeatedly, may result in molecular "blinking" (see Chapter 8). A further pathway to leave S_1 or T_1 is by photobleaching. Photobleaching is the irreversible destruction of the molecule, which is often accompanied by the production of reactive and toxic molecular species.

the energy of the molecule is still higher than in the electronic ground state, the S_1 state is not stable for a long time, but the molecule will return to the ground state S_0. The time spent in S_1 is designated as excited state lifetime τ. Highly fluorescent molecules return to the ground state upon emitting the excess energy as light – emission of a *fluorescence photon*. This again changes the electronic configuration around the nuclei and therefore this decay to the electronic ground state ends in a vibrational excited state. From here, the molecule again rapidly returns to the vibrational ground state of S_0 by dissipating the vibrational energy to the surroundings. Now the fluorescence cycle is completed.

It should be noted that the decay from S_1 to S_0 may also happen as a result of further collisions with solvent molecules, by which the electronic excess energy is lost. In this case, no fluorescence photon is emitted, and therefore this process is designated as *nonradiative decay*. Finally, a third decay pathway is relaxation via *intersystem crossing*. It exists because the excited electron has a certain, but usually very small, probability to flip its spin and thus to reach another state with a slightly lower energy, the so-called triplet state, designated as T_1. In order to return from T_1 back into the electronic ground state S_0, it needs to flip its spin a second time, because in S_0 it needs the antiparallel spin to the second electron to share the same molecular orbital. Again, this is an improbable and therefore slow process occurring on time scales of microseconds up to even hours. This may happen upon emission of a photon, a process that is designated as *phosphorescence*. However, often the radiative decay cannot compete with nonradiative pathways. A summary of the excitation and various decay pathways is usually given in form of a so-called Jablonski diagram (Figure 3.1).

It should be noted that even the longest absorption wavelength, corresponding to excitation from the lowest vibrational level of S_0 to the lowest vibrational level of S_1, and the shortest wavelength emission, corresponding to de-excitation between the same levels, occur at different wavelengths because reorientation of neighboring solvent molecules within the lifetime of the excited state lowers the energy of the excited state and raises that of the ground state, thereby decreasing the energy of the emitted photon. The process of the reorientation of the solvent molecules is designated as *solvent relaxation*. Altogether, the difference between the peak wavelengths of absorption and emission is designated as *Stokes shift*. It is due to solvent relaxation and to the loss of the vibrational energies in S_1 and S_0.

Box 3.1 Kinetics and Equilibrium Properties of Fluorescence Emission

A very powerful approach to the kinetics of fluorescence emission is to neglect the details of the vibrational states and just to analyze the transitions between the various electronic molecular states. These transitions can be formulated in the language of chemical kinetics. For an ensemble of molecules, we can describe the populations of molecules in S_0, S_1, and T_1 as $[S_0]$, $[S_1]$, and $[T_1]$. For simplicity, we consider only transitions from S_0 to S_1 and neglect excitation to higher states, for example, S_2. If we use the rates for the transitions between the various states as denoted in Figure 3.1, we can describe the time-dependent populations of the

states as follows:

$$\frac{d[S_0]}{dt} = -k_{exc}[S_0] + (k_f + k_{nr})[S_1] + k_p[T_1] + k_{nrT}[T_1] \tag{3.1a}$$

$$\frac{d[S_1]}{dt} = k_{exc}[S_0] - (k_f + k_{nr} + k_{isc})[S_1] \tag{3.1b}$$

where $k_{exc} = I_{exc}\sigma_a$, I_{exc} denotes the exciting photon flux, and σ_a is the absorption cross section of the fluorophore at the respective wavelength. This set of equations can be used to calculate the steady-state distribution of the ensemble by setting all derivatives to zero. Also, the same equations can be used to predict the time dependent decay of $[S_1]$ after a short excitation pulse, causing a certain population of S_1, $[S_1]_0$. In that case, integration of Eq. (3b) over time yields

$$[S_1(t)] = [S_1]_0 e^{-(k_f+k_{nr}+k_{isc})\,t} \tag{3.2}$$

and we see that the return to the ground state is described by a mono-exponential function $e^{-t/\tau}$, and the excited state lifetime τ is given as

$$\tau = \frac{1}{k_f + k_{nr} + k_{isc}} \tag{3.3}$$

The relative probability of a specific transition is given by that rate divided by the sum of all rates describing the decay from that state. For example, the probability of emitting a fluorescence photon after excitation into S_1, also called the *quantum efficiency* Φ, is given by

$$\Phi = \frac{k_f}{k_f + k_{nr} + k_{isc}} \tag{3.4}$$

For one of the most efficient fluorophores, phycoerythrin, this value is nearly unity (0.98). Finally, the amount of emitted fluorescence photons per second is given by the fluorescence rate k_f times the population $[S_1]$ of molecules in state S_1.

3.2.2 Fluorescence Excitation and Emission Spectra

The energy of the exciting photon must be high enough so that the molecule can cross the energy gap between ground state S_0 and excited state S_1. This energy gap is quite broad, however, because the molecule usually ends in a vibrational excited state of S_1. The energy gap is the reason why only absorption of photons with a certain minimum energy will lead to a molecular excitation. In a molecular ensemble, numerous effects further slightly alter the spectral transition energies, that is, additional translational and rotational energy levels and different molecular surroundings. Therefore, at room temperature molecules absorb and emit light within a continuous spectrum of energies rather than at sharp spectral lines. The energy or wavelength dependence of the fluorescence excitation is usually plotted in the form of a fluorescence excitation spectrum. This is a plot of the intensity of the emitted fluorescence measured at a specific emission wavelength as a function of the excitation wavelength. The fluorescence emission spectrum, on the other hand, shows the fluorescence intensity as a function of the emission wavelength when exciting a sample at a selected wavelength in the absorption

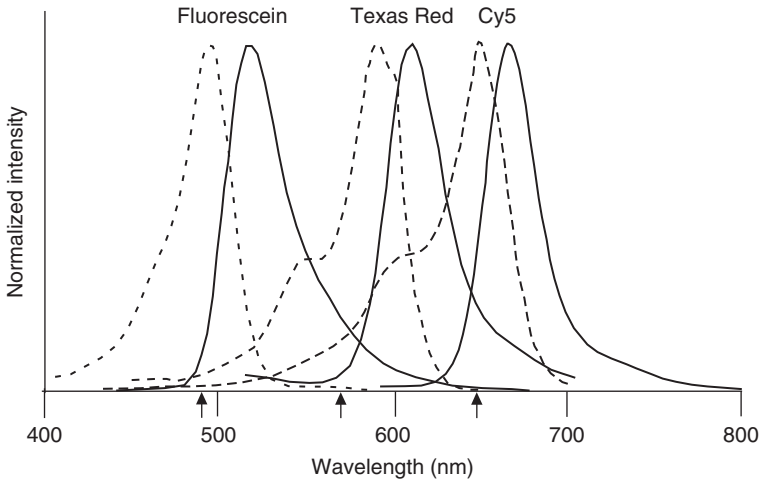

Figure 3.2 Fluorescence excitation (dashed lines) and emission (full lines) spectra of heterocyclic compounds fluorescein, Texas Red, and Cy5. The arrows indicate the wavelengths of laser lines that are often used in microscopy to excite these dyes.

band. For single molecules, both excitation and emission spectra represent probability densities of excitation and emission.

The fluorescence excitation and emission spectra for three typical dyes, fluorescein, Texas Red, and Cy5, are shown in Figure 3.2. There is one characteristic maximum in each excitation spectrum corresponding to the energy gap between the vibrational ground state of S_0 and the vibronic level of S_1 to which the transition is most probable. All three excitation spectra show a shoulder on the blue side, which is due to molecular transitions to a higher vibrational state of S_1. The fluorescence emission spectra are usually approximate mirror images of the excitation spectra because the decay occurs from the vibrational ground state of S_1 to levels of S_0 having overall a similar structure as in S_1. The magnitude of the respective Stokes shifts can be deduced directly from the spectra.

3.3 Features of Fluorescence Microscopy

3.3.1 Image Contrast

In full daylight, it is almost impossible to spot a firefly against the background of grasses, bushes, and trees at the edge of a forest. At night, however, the same firefly glows and thus becomes visible to an observer, while the plants and numerous other insects that might be active in the same area are completely undetectable. This example parallels, to some degree, the observation of a selected molecule under a fluorescence microscope. To be useful for an investigator, optical microscopy requires high *contrast*. This condition is fulfilled well by fluorescence microscopy, where selected molecules are incited to emit light and stand out against a black background (Box 3.2), which embraces a countless number of other molecules in the investigated cell (Figure 3.3).

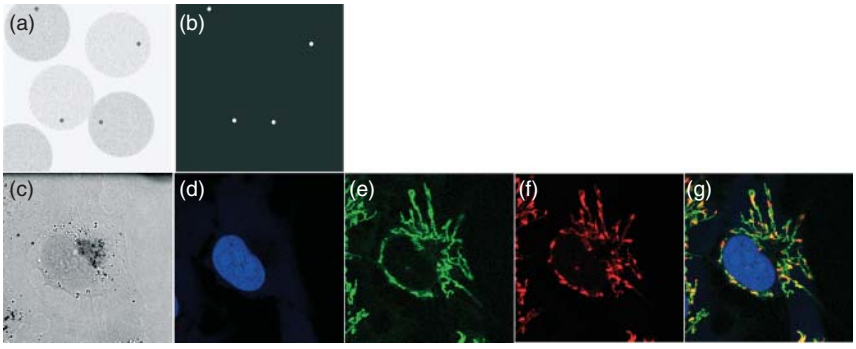

Figure 3.3 Importance of image contrast in microscopy. (a) Four dark-gray dots are almost undetectable against a light-gray background. (b) Four white dots, in the same positions as in (a), are easily discerned against a black background. (c) A transmitted light image of a live cell in culture – almost no internal features can be distinguished when no contrasting technique is used. (d) Nuclear DNA stained with DAPI; DAPI is a heterocyclic molecule with affinity for DNA. The major mode of binding to DNA is thought to be dependent on positioning a DAPI molecule in a minor groove of a double helix. (e,f) Low (green, e) and high (red, f) potential mitochondria fluorescently labeled with JC-1. JC-1 is a carbocyanine dye, which readily crosses plasma and mitochondrial membranes and is accumulated inside active mitochondria. JC-1 monomers emit green fluorescence. At high concentrations (above 0.1 μM in solution), JC-1 forms the so-called J-aggregates emitting red luminescence. A gradient of electric potential is responsible for the passage of JC-1 molecules across the membranes into active mitochondria. Mitochondria characterized by a high membrane potential accumulate JC-1 and the dye reaches the concentration that is sufficiently high to form J-aggregates. (g) Fluorescence signals from mitochondria and nucleus overlaid in one image. (Images (c)–(g) courtesy of Dr A. Waligórska, Jagiellonian University.)

Box 3.2 Discovery of Fluorescence

Fluorescence was first observed by an English mathematician and astronomer, Sir John Frederick William Herschel, probably around 1825. He observed blue light emitted from the surface of a solution of quinine. Sir John was a man of many talents. He made important contributions to mathematics, astronomy, and chemistry, authored inventions pertinent to early photography, published on the photographic process and was the first one to use the fundamental terms of analog photography – "a negative" and "a positive." He is thought to have influenced Charles Darwin. In 1845, Herschel described this observation in a letter to The Royal Society in London:

> A certain variety of fluor spar, of a green colour, from Alston Moor, is well known to mineralogists by its curious property of exhibiting a superficial colour, differing much from its transmitted tint, being a fine blue of a peculiar and delicate aspect like the bloom on a plumh…

(Continued)

Box 3.2 (Continued)

He found a similar property in a solution of quinine sulfate:

> …Though perfectly transparent and colourless when held between the eye and the light, or a white object, it yet exhibits in certain aspects, and under certain incidences of the light, an extremely vivid and beautiful celestial blue color, which, from the circumstances of its occurrence, would seem to originate in those strata which the light first penetrates in entering the liquid… [1].

In the next report, he referred to this phenomenon as *epipolic dispersion* of light [2]. Herschel envisaged the phenomenon he saw in fluorspar and quinine solution as a type of dispersion of light of a selected color.

In 1846, Sir David Brewster, a Scottish physicist, mathematician, and astronomer, well known for his contributions to optics, and numerous inventions, used the term *internal dispersion* in relation to this phenomenon.

In 1852, Sir John Gabriel Stokes, born in Ireland, a Cambridge University graduate and professor, published a 100 page long treatise "On the Change of Refrangibility of Light" [3] about his findings related to the phenomenon described by Sir John Herschel. He refers to it as "dispersive reflection." The text includes a short footnote, in which Stokes said:

> I confess I do not like this term. I am almost inclined to coin a word, and call the appearance *fluorescence*, from fluor-spar, as the analogous term opalescence is derived from the name of a mineral.

It was known at that time that when opal was held against light, it appeared yellowish red; however, when viewed from the side, it appeared bluish. Thus, the phenomenon was similar to the one observed by Herschel in fluorspar. We now know that opalescence is a phenomenon related to light scattering, while the phenomenon seen in a solution of quinine was not exactly a dispersion of light of a selected wavelength, but rather the emission of a light of a different color. Sir J. G. Stokes is remembered for his important contributions to physics, chemistry, and engineering. In fluorescence, the distance, in wavelength, between the maximum of excitation and emission is known as *Stokes shift*.

The physical and molecular basis for the theory of fluorescence emission was formulated by a Polish physicist Aleksander Jabłoński [4]. Hence, the energy diagram that describes the process of excitation and emission of fluorescence is called the *Jabłoński diagram* (Figure 3.1). Aleksander Jabłoński was a gifted musician; during his PhD years, he played the first violin at the Warsaw Opera. In postwar years, he organized a Physics Department at the University of Toruń in Poland and worked there on various problems of fluorescence.

The range of applications of fluorescence microscopy was originally underestimated. Fluorescence microscopy was seen as just a method of obtaining nice, colorful images of selected structures in tissues and cells. The most attractive

feature of contemporary fluorescence microscopy and many modern imaging and analytical techniques, which grew out of the original idea, is the ability to image and study quantitatively not only the structure but also the function, that is, physiology, of intact cells *in vitro* and *in situ*.

Figure 3.3 illustrates the fact that modern fluorescence microscopy should not be perceived merely as a technique of showing enlarged images of cells and subcellular structures but as a way of studying cellular functions. Figure 3.3e–g shows some selected structures within a cell (mitochondria and the cell nucleus) and demonstrate the ability to selectively convert a physiological (functional) parameter – in this case, mitochondrial potential – into a specific fluorescence signal.

3.3.2 Specificity of Fluorescence Labeling

Let us expand the analogy of the firefly. Although one does not see any features of the firefly – its size, shape, or color remain unknown – the informed observer knows that the tiny light speckle that reveals the position of a male firefly. It is most likely a European common glowworm, *Lampyris noctiluca*. No other insects are expected to emit light while flying in this region at this time of the year. Although there may be hundreds of insects hovering in this place, they blend into the black background and therefore are not visible. Thus, a tiny light label is characteristic of a firefly: it is specific. *Specificity* of fluorescence labeling of selected molecules of interest as well as specificity of translating some selected physiological and functional parameters such as membrane potential or enzyme activity into specific signals in a cell is another important advantage of fluorescence microscopy (Figures 3.3 and 3.4). Hundreds of fluorescent molecules, both small heterocyclic molecules and proteins, are available to be used as specific labels and tags in fixed and live cells. Also, a host of methods have been optimized for attaching a fluorescent tag to a molecule of interest; they are discussed in Chapter 4.

Specificity of labeling is an important advantage of fluorescence microscopy. However, this specificity is never ideal and should not be taken for granted. Let us consider the example given in Figure 3.4. DRAQ5 binds DNA fairly specifically; staining of RNA is negligible owing to either a low binding constant or a low fluorescence intensity of the DRAQ5 complex with RNA, as long as the concentration of DRAQ5 is low. At high DRAQ5 concentrations, when all binding sites for the dye on DNA are saturated, some binding to RNA can be detected. A similar phenomenon is observed with most, if not all, fluorescent labels that exhibit affinity for DNA. Thus, experimental conditions, especially the ratio between the available dye and the available binding sites, have to be optimized in order to fully exploit the advantages of the DNA-labeling techniques. As for Col-F, this small molecule binds to two major components of the extracellular matrix; in this respect, it is less specific than antibodies directed against selected epitopes on collagen or elastin in a selected species. The advantage of Col-F is the simplicity of labeling, deep tissue penetration, and low level of nonspecific staining. The advantage of immunofluorescence in the detection of collagen or elastin is its very high specificity, but it comes with limitations: shallow

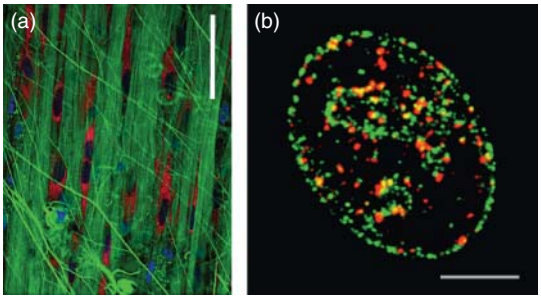

Figure 3.4 Specificity of fluorescence labeling. (a) Three fluorescent probes were used to stain different classes of molecules and structures in a fragment of live connective tissue – DNA in cell nuclei (DRAQ5, a deep-red emitting dye, shown here as blue), fibers of the extracellular matrix (Col-F, green), and active mitochondria (tetramethylrhodamine abbreviated as TMRE, red). Scale bar, 50 μm. DRAQ5 is an anthracycline derivative that has high affinity for DNA. The dye readily crosses plasma and nuclear membranes and binds to DNA in live cells. It is optimally excited by red light, emitting in deep red. Here, it is shown as blue to be distinguished from TMRE. Col-F is a dye that binds to collagen and elastin fibers (excitation – blue, emission – green). TMRE enters cells and is accumulated by active mitochondria (excitation – green, emission – red). (b) A DNA precursor analog, ethylenedeoxyuridine (EdU), was incorporated into nascent DNA during a short period of S-phase in the division cycle, in cells exposed to an inhibitor of topoisomerase type I, camptothecin. Cells were fixed and the EdU was labeled fluorescently using "click chemistry." Newly synthesized DNA is thus marked in green. In the same cell, γH2AX, a phosphorylated form of histone H2AX, which is considered a marker of DNA double-strand breaks (DSBs), was labeled using a specific antibody. Thus, DNA regions with DSBs are immunolabeled in red. When images of numerous foci representing DNA replication and DNA damage are overlaid, it becomes apparent that most damage occurred in replicating DNA (replication and γH2AX foci show large yellow areas of overlapping green and red signals). Scale bar, 5 μm. (Biela et al. [23] and Berniak et al. [24].)

penetration into tissue and some nonspecific binding of the fluorescently labeled secondary antibody used in the labeling method. An experimenter has to make a choice between the advantages and limitations of the low molecular weight label and the immunofluorescence approach. Similarly, Figure 3.4b shows two labeling methods that differ to some degree in their specificity. Incorporating precursors ethylenedeoxyuridine (EdU) into nascent DNA and subsequently labeling the incorporated molecules (the click reaction) leads to a very specific labeling of newly synthesized DNA, with very low or even no background staining. Labeling the phosphorylated moieties of histone H2AX with specific antibodies is very specific, but some nonspecific binding by a secondary antibody cannot be avoided. Consequently, a low-level fluorescence background is usually present.

A very high level of specificity is provided by genetic manipulation of cells, leading to expression of fluorescently tagged proteins (Chapter 4).

3.3.3 Sensitivity of Detection

Contemporary fluorescence microscopy offers highly sensitive detection of fluorescent species. The advent of highly sensitive light detectors and cameras made

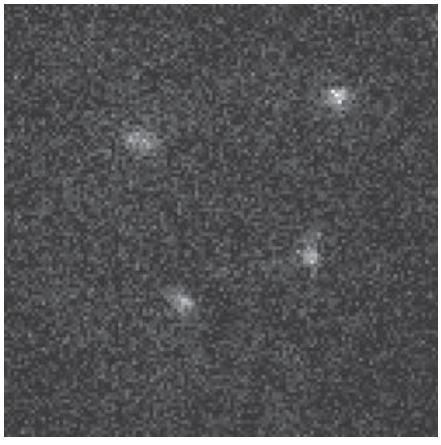

Figure 3.5 Single molecules of a fluorescent lipid tracer, TopFluor-PC, in lipid bilayers, imaged with an electron-multiplying CCD (EMCCD) camera. Each molecule produces a diffraction-limited signal as discussed in Chapter 2 (field of view, $10 \times 10\ \mu m^2$). (Image courtesy of Katharina Scherer, Bonn University.)

it possible to detect even single molecules in the specimen (Figure 3.5). Thus, the observation of single-molecule behavior, such as blinking, or the detection of interactions between individual molecules by Förster resonance energy transfer (FRET) has become possible.

The analogy between watching a fluorescent molecule under a microscope and a firefly at night still holds when one thinks of the size and shape of a firefly. A small spot of fluorescent light seen through a microscope may represent one molecule. Although the observer can identify the position of the molecule in space and can watch its movement, the shape and size of this molecule remain unknown (Figure 3.5). Despite this limitation, the ability to detect single molecules opened the way to a number of interesting new techniques, including speckle microscopy and, most importantly, super-resolution methods (see sections below and Chapters 8 and 12).

3.4 A Fluorescence Microscope

3.4.1 Principle of Operation

The analogy between a firefly and a fluorescent object, which was useful in introducing basic concepts, ends when one considers the instrumentation required to detect fluorescence in a microscope. While a firefly emits light on its own by a biochemical process called *bioluminescence*, which uses energy from adenosine triphosphate (ATP), but does not require light to be initiated, the fluorescence in a microscopic object has to be excited by incident light of a shorter wavelength. Thus, a fluorescence microscope has to be constructed in a way that allows excitation of fluorescence, subsequent separation of the relatively weak emission from the strong exciting light, and, finally, detection of fluorescence. An efficient separation of the exciting light from the fluorescence light, which eventually reaches the observer's eye or the electronic detector, is mandatory for obtaining high image contrast. A sketch of a standard widefield fluorescence microscope is shown in Figure 3.6.

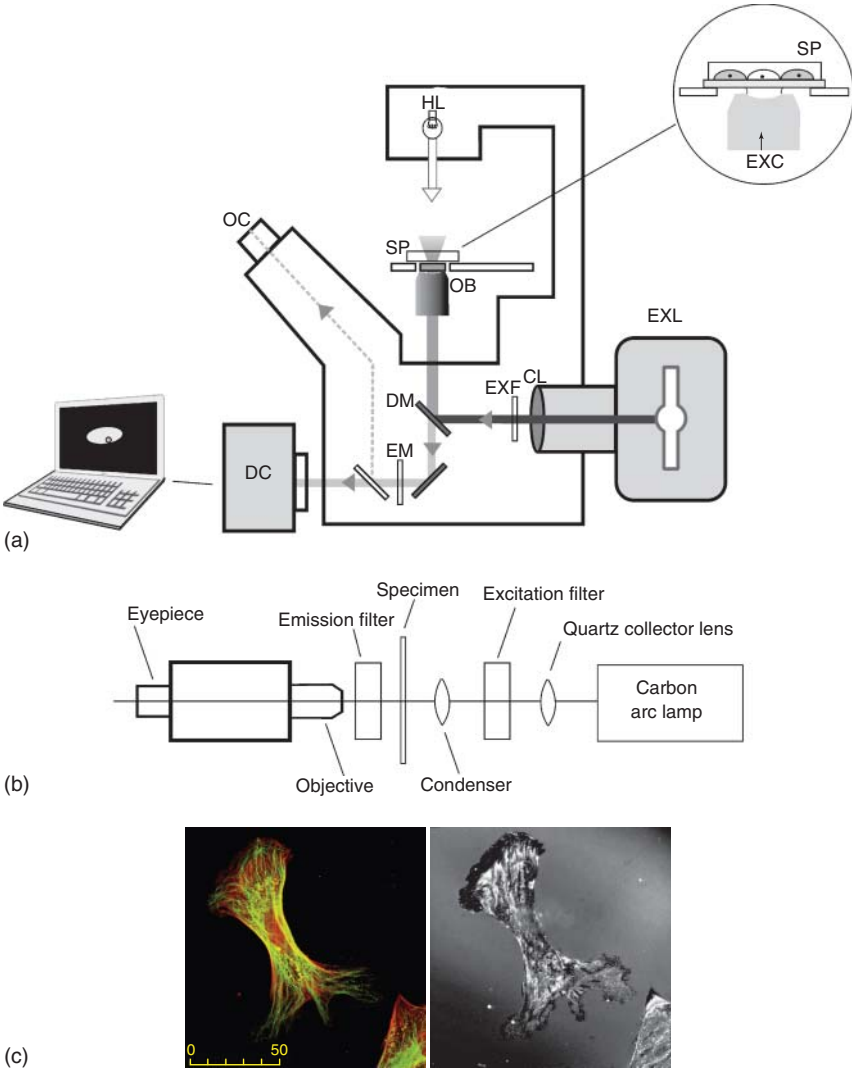

Figure 3.6 Fluorescence microscope – principle of operation. (a) A schematic diagram of an inverted fluorescence microscope (epifluorescence). This type of microscope enables studies of live cells maintained in a standard growth medium, in tissue culture vessels, such as Petri dishes. HL, halogen lamp; SP, specimen; OB, objective lens; OC, ocular lens (eyepiece); DC, digital camera; EXL, exciting light source; CL, collector lens; EXF, excitation filter; DM, dichroic mirror; EM, emission filter; EXC, exciting light incident on the specimen. (b) A schematic diagram of an early fluorescence microscope, with dia-illumination. (c) Fluorescence images of microtubules (green) and actin fibers (red) and an image of the same cell in reflected light (Box 3.3), demonstrating focal contacts (black). (Images by J. Dobrucki, Jagiellonian University, Kraków.)

Box 3.3 Reflected Light Imaging

The epifluorescence design makes it possible to detect reflected light. In this mode of observation, a dichroic mirror is replaced with a silver-sputtered mirror that reflects and transmits the incident light in desired proportions; also the emission filter has to be selected to allow the reflected exciting light to enter the detector (additional optical components are needed to minimize the effects of light interference). Imaging reflected light adds another dimension to fluorescence microscopy. Figure 3.6c shows an example of reflected light imaging – visualization of focal contacts in a fibroblast attached to a glass surface. The images were collected in a confocal fluorescence microscope that was set up for two-channel fluorescence and reflected light imaging.

Fluorescence is excited by light that is emitted by a mercury lamp. The exciting light is reflected toward the sample by a dichroic (two-color) mirror (Figures 3.6 and 3.7). This special mirror is positioned at 45° angle toward the incoming light and reflects photons of a selected wavelength but allows those of longer wavelengths to pass through. The dichroic mirror is selected for a given application; that is, it is made to reflect the chosen exciting wavelength and allow the passage of the expected fluorescence (Figure 3.8). It is important to realize that the efficiency of converting exciting light into fluorescence is usually low, that is, only one out of many exciting photons is converted into a photon

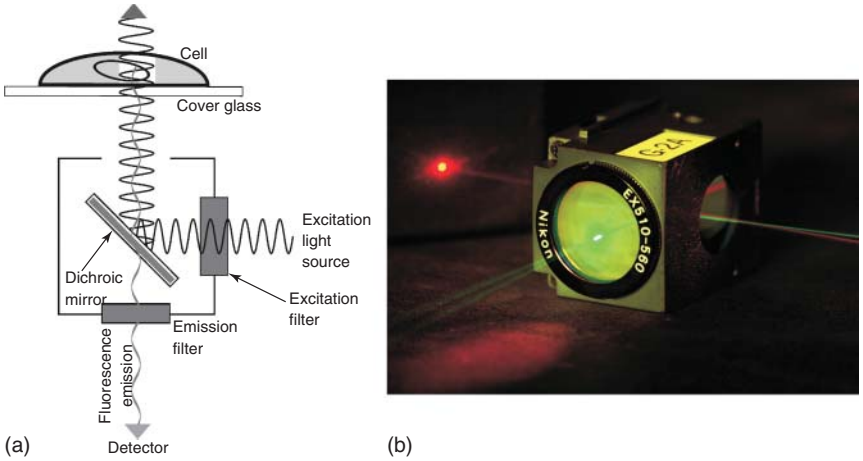

Figure 3.7 A fluorescence microscope filter block. (a) A schematic diagram of a typical filter block containing an excitation filter, a dichroic mirror, and an emission filter. The exciting light emitted by a light source is reflected by the dichroic mirror toward the specimen; the fluorescence emission has a longer wavelength than the exciting light and is transmitted by the dichroic mirror toward the ocular lens or a light detector. (b) A photograph of a microscope filter block, which reflects green but transmits red light. The excitation filter is facing the observer and the dichroic mirror is mounted inside the block; the emission filter (on the left side of the block) cannot be seen in this shot. Light beams emitted by laser pointers were used. In a fluorescence microscope, the intensity of the red emission would be significantly lower than the intensity of the exciting green light. (Photograph by J. Dobrucki.)

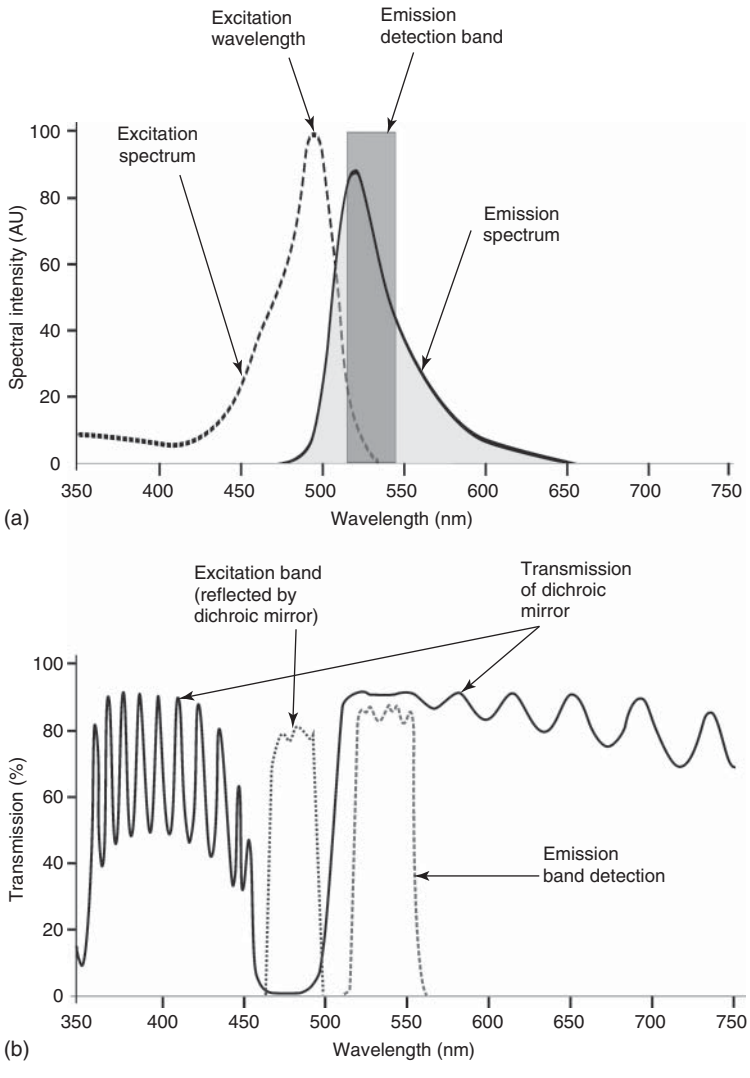

Figure 3.8 Spectral properties of a typical fluorescent label, fluorescein (a), and the characteristics of a filter set suitable for selecting the excitation band and detecting fluorescence emission (b).

of a longer wavelength and subsequently detected as fluorescence. Moreover, fluorescence is emitted by the sample in all directions, but only a selected light cone, that is, a fraction of this fluorescence, is collected by the objective lens. Consequently, fluorescence is weak in comparison with the exciting light and has to be efficiently separated and detected. High-quality optical filters are used to select exclusively the desired exciting wavelength (excitation filter) and the fluorescence emission bands (emission filter) (Figure 3.7). It is worth noting that the arrangement described here, called *epifluorescence* (which resembles the reflected light microscope that is used in studies of metal surfaces), makes

it relatively easy to separate the fluorescence from the exciting light. It is also safer for the operator than an original dia-illumination system. In the early days of fluorescence microscopy, a direct (dia-)illumination of the sample was used (Figure 3.6b). The exciting light was prevented from reaching the observer only by virtue of placing an efficient blocking filter in the light path.

In the original fluorescence microscope design, removing the excitation filter from the light path allowed the intense exciting light into the eyepiece and the eyes of the observer. Even in the case where the objective lens does not allow UV light to pass through, this would be very dangerous. In the epifluorescence design, there is no danger of sending the exciting light directly into the eyes of the observer. Even when the dichroic and excitation filters are removed, the exciting light will not be incident directly onto the ocular lens. This does not mean, however, that it is safe to look through the microscope with the exciting light source turned on and all the filter blocks removed out of the light path. When filters are removed, the exciting light is still sufficiently reflected and scattered to pose a hazard to the eyes of the observer. To protect one's lab-mates, if filter blocks are removed, it is advisable to leave an appropriate note to warn others who might come to "only have a brief look at their sample."

3.4.2 Sources of Exciting Light

A typical fluorescence microscope contains two sources of light. One, usually a halogen lamp, is used for initial viewing of a specimen in the transmitted light mode. Another, often a mercury arc lamp, is used for exciting fluorescence. Halogen lamps belong to a class of incandescent (or "candescent") light sources, where the emission of photons occurs through the heating of a tungsten filament. High-pressure mercury vapor arc-discharge lamps (HBO) are a popular source of exciting light in standard fluorescence microscopes. The intensity of light emitted by a mercury arc lamp is up to 100 times greater than that of a halogen lamp. The spectrum of emission, shown in Figure 3.9a, extends from the UV to the infrared. The spectrum depends to some degree on the pressure of the mercury vapor and on the type of lamp. The desired excitation spectral band is selected by using an appropriate excitation filter. As the spectrum consists of numerous sharp maxima, the intensity of the exciting light strongly depends on the selected wavelength. Mercury arc lamps are very convenient sources of excitation for a number of typical fluorophores. Another popular source of exciting light is a xenon arc lamp. It emits an almost continuous spectrum of emission in the whole range of visible wavelengths (Figure 3.9b). Metal halide lamps are a modification of mercury vapor lamps, characterized by higher levels of emission between the major mercury arc spectral lines (Figure 3.9c) and a much longer lifetime. Here, the spectrum is dependent on the metal used for doping.

The stream of photons emitted by the filament in the bulb is not ideally uniform in space or constant in time. It has been demonstrated that a hot light source emits groups (bunches) of photons, rather than individual, independent photons. This intriguing phenomenon (photon bunching) was observed in a classical physics experiment performed by Hanbury Brown and Twiss (for a discussion

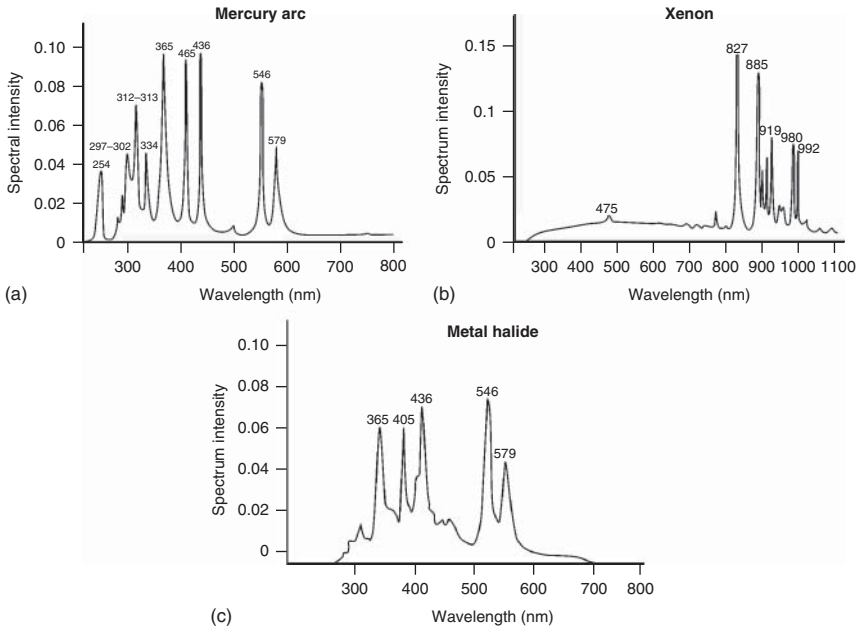

Figure 3.9 Schematic diagrams of the emission spectra of (a) a mercury arc, (b) a xenon lamp, and (c) a metal halide lamp. (Figure by M. Davidson, Microscopy Primer, University of Florida, with permission, redrawn.)

of photon bunching and the relation of this phenomenon to the corpuscular and wave nature of light, see [5]). There are also more trivial sources of spatial and temporal inhomogeneity of emitted light, including fluctuations in the temperature of the filament, instability of the electric current, and the influence of external electromagnetic fields. Consequently, the popular mercury arc lamps pose some problems for quantitative microscopy. The illumination of the field of view is not uniform, and the intensity of light fluctuates on a short time scale that is comparable with the times needed to record pixels and images and it diminishes over days of the lamp use because the electrodes are subject to erosion. Thus, quantitative fluorescence microscopy studies are hampered by the lack of short- and long-term stability of the exciting light. A higher stability of emission is offered by light-emitting diodes (LEDs) and laser light sources.

A typical HBO burner needs to be placed exactly at the focal point of the collector lens (when exchanging HBO burners, the quartz bulb must not be touched by fingers). Centering is important to ensure optimal illumination, that is, the highest attainable and symmetric illumination of the field of view. After being turned off, HBO burners should be allowed to cool before switching them on again. They should be exchanged upon reaching the lifetime specified by the manufacturer (usually 200 h). Using them beyond this time not only leads to a significantly less intensive illumination but also increases the risk of bulb explosion. Although relatively rare, such an event may be costly, as the quartz collector lens located in front of the burner may be shattered. HBO burners need to be properly disposed of to avoid contamination of the environment with

mercury. Today's metal halide lamps are usually pre-centered and fixed in the optimal position in the lamp housing.

Lasers emit light of discrete wavelengths, characterized by high stability both spatially (the direction in which the beam is propagated is fixed; so-called beam-pointing stability), and temporally – both on a short and long timescale.

In the early days of fluorescence microscopy, lasers did not exist; subsequently, their use was limited to laser scanning microscopes, which were more advanced and more expensive than standard widefield fluorescence microscopes (Chapter 5). The stability of the light beams and the ability to focus them to a diffraction-limited spot were important advantages of lasers over mercury arc lamps. The disadvantages, however, were their high cost and the limited number of usable emission lines for exciting popular fluorophores. For instance, the popular 25 mW argon ion laser provided the 488 and 514 nm lines, which were not optimal for working with the most popular (at that time) pair of fluorescent dyes – fluorescein and rhodamine. Other gas lasers that are often used in confocal fluorescence microscopy include krypton–argon (488, 568, and 647 nm) and helium–cadmium (442 nm). Solid-state lasers, including a frequency-doubled neodymium-doped yttrium aluminum garnet (Nd:YAG, 532 nm), are also used.

Currently, the price of standard gas lasers has decreased, and a wide selection of various single-line lasers as well as lasers emitting a broad wavelength spectrum are available, including a "white light laser." Durable diode lasers have become available as well. Moreover, new low-cost sources of light, LEDs, have become available. LEDs are semiconductors that exploit the phenomenon of electroluminescence. Originally used only as red laser pointers, they now include a range of devices emitting in UV, visible, or NIR spectral region. The critical part of an LED is the junction between two different semiconducting materials. One of them is dominated by negative charge (n-type) and the other by positive charge (p-type). When voltage is applied across the junction, a flow of negative and positive charges is induced. The charges combine in the junction region. This process leads to a release of photons. The energy (wavelength) of these photons depends on the types of semiconducting materials used in the LED. A set of properly selected LEDs can now be used as a source of stable exciting light in a fluorescence microscope. LEDs are extremely durable, stable, and are not damaged by being switched on and off quickly. These advantages are making them very popular not only in scanning confocal microscopes but in standard fluorescence microscopes as well.

3.4.3 Optical Filters in a Fluorescence Microscope

In a fluorescence microscope, light beams of various wavelengths need to be selected and separated from each other by means of optical glass filters. The filter that selects the desired wavelength from the spectrum of the source of exciting light is called an *excitation filter*. There is also a need to control the intensity of the exciting light. This can be achieved by placing a neutral density filter in the light path, if it is not possible to regulate the emission intensity directly. Fluorescence is emitted in all directions; most of the exciting light passes straight through

the specimen, but a large part is scattered and reflected by cells and subcellular structures. A majority of the reflected exciting light is directed by the dichroic mirror back to the light source, while a selected wavelength range of the emitted fluorescence passes through toward the ocular lens or the light detector. In a standard widefield fluorescence microscope, the emission filter is mounted on a filter block, which is placed in the light path to select the desired emission bandwidth. If only one set of spectral excitation and emission wavelengths were available in a microscope, the applicability of the instrument would be seriously limited, as only one group of spectrally similar fluorescent probes could be used. Therefore, a set of several filter blocks prepared for typical fluorescent dyes is usually mounted on a slider or a filter wheel. This allows for a rapid change of excitation and emission ranges. In fluorescence confocal microscopes, the dichroic filter is often designed so as to reflect two or three exciting wavelengths and transmit the corresponding emission bands. Additional dichroic mirrors split the emitted light into separate beams directed toward independent light detectors. This makes it possible to simultaneously excite and observe several fluorophores. Some widefield fluorescence microscopes incorporate electronically controlled excitation and emission filter wheels, which contain sets of several optical filters. The desired combination of filters can be quickly selected using a software package that drives the filter wheels and the shutters.

Although microscope manufacturers offer standard filter blocks for most popular fluorescent probes, it is useful to discuss and order custom-made filter sets optimized for the source of exciting light and for the user's specific applications. It is also prudent to buy an empty filter block (holder) when purchasing a new microscope, in order to make it possible to build one's own filter blocks when new applications are desired. "In-house" assembling one's own filter block may require some skill and patience, because the position of the dichroic mirror in relation to the beam of exciting light is critical. Microscope manufacturers provide filter blocks with dichroic filters fixed in the optimal position. Aligning the dichroic mirror by the user should be possible, but may be cumbersome in some microscopes. When buying individual filters, especially dichroics, it is important to choose high-quality filters, that is, low-wedge filters (flat, with both surfaces ideally parallel), with the smallest number of coating imperfections. Defects in coating will allow the exciting light to reach the fluorescence detector. The exciting light reaching the detector will be detected as a background, thereby reducing the contrast and degrading image quality. Also, when buying dichroics in order to build one's own filter combinations, it is important to ensure that not only the shape and diameter but also the thickness of the filter is right for a given microscope design. Aligning a dichroic filter of a different thickness may turn out to be impossible. The orientation of a dichroic filter in relation to the incident light is important – the surface of the interference filter that should face the light source is specified by the manufacturer (note that the arrow can mean the direction of light propagation or the direction toward the light source, depending on the manufacturer). Optical filters have to be handled with care to avoid leaving fingerprints, grease, and dust on the surface. Newer hard-coated filters are quite robust and easier to clean. If cleaning is required, it can be done by blowing air

or using a soft brush (to remove the dust) and subsequently using a piece of optical tissue (the tissue is not to be reused) with a small amount of pure methanol or isopropyl alcohol. The manufacturer of the filter will usually recommend the solvent that is appropriate for their products. It is important to ensure that the antireflection coating is not scratched or damaged.

The state of current technology in the manufacturing glass optical filters is so advanced that filters of various optical characteristics can be custom-made by the optical companies.

3.4.4 Electronic Filters

A new class of versatile optoelectronic elements that serve as filters has become available in recent years. These include the acousto-optic tunable filters (AOTFs). They provide flexibility and speed in choosing light wavelength and intensity that cannot be achieved with glass optical filters. This flexibility and speed is indispensable in modern advanced fluorescence confocal microscopes.

AOTFs work in a manner similar (though not identical) to a diffraction grating. A specialized birefringent crystal is subjected to high-frequency (a few hundred megahertz) acoustic waves that induce a periodic pattern of compression (Figure 3.10). This, in turn, changes the local diffractive index of the crystal and imposes a periodic pattern of different refractive indices. Most AOTFs use tellurium dioxide (TeO_2). This material is transparent in the range of 450–4000 nm. Only a selected band from a whole range of light wavelengths incident on the crystal is deflected. In this respect, the crystal resembles a band-pass filter rather than a diffraction grating where a whole range of wavelengths are diffracted (at different angles). The direction in which the light beam is deflected is fixed and does not depend on the wavelength. The wavelength of the diffracted band depends on the frequency of the acoustic

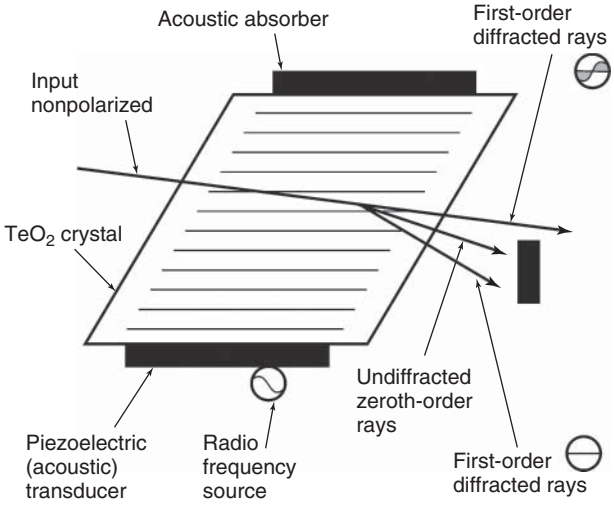

Figure 3.10 Architecture and principle of operation of an acousto-optic tunable filter (AOTF). (Lichtmikroskopie online, Vienna University, modified.)

wave. The intensity of the deflected light can be controlled by the amplitude of the acousto-mechanical wave incident on the crystal. The wave is impressed onto the crystal by a piezoelectric transducer, which is a device that expands and shrinks according to the applied voltage. AOTFs can be used to rapidly change the wavelength as well as the intensity of the deflected light by changing the frequency and the amplitude of the incident acoustic waves that drive the crystal. The spectral width of the deflected light can be controlled by delivering multiple frequencies to the AOTF. Moreover, using several widely spaced frequencies will allow a set of wavelength bands to be deflected at the same time. These characteristics make AOTF a flexible component of a fluorescence microscope, which can serve simultaneously as a set of fast shutters, neutral density filters, and emission filters, allowing simultaneous detection of several emission colors. Changing the wavelengths and their intensity can be achieved at a high speed, namely, tenths of microseconds, while filter wheels need time on the order of a second. An AOTF can also be used as a dichroic filter, which separates the exciting light from fluorescence emission. These advantages make AOTFs particularly valuable for multicolor confocal microscopy and techniques such as fluorescence recovery after photobleaching (FRAP, [6] chapter 11).

3.4.5 Photodetectors for Fluorescence Microscopy

In most microscopy applications, there is a need to record fluorescence images – often a large number of images within a short time – for subsequent processing, analysis, and archival storage. Originally, analog recording of fluorescence images on a light-sensitive film was extensively used, but in the past two decades methods of electronic detection, analysis, and storage have become efficient and widely available. Currently, fluorescence microscopes are equipped with suitable systems for light detection, image digitization, and recording. The most common light detector in a standard widefield fluorescence microscope is a charge-coupled device (CCD) camera, while photomultipliers are used in laser scanning confocal microscopes. Other types of light detectors, including intensified charge-coupled device (ICCD) and electron multiplied charge-coupled device (EMCCD) cameras, as well as avalanche photodiodes (APDs), are gaining increasing importance in modern fluorescence microscopy.

3.4.6 CCD or Charge-Coupled Device

In a camera based on a CCD, an image is projected onto an array of semiconducting, light-sensitive elements that generate an electric charge proportional to the intensity of the incident light (Figure 3.11). Two types of sensor architectures are currently produced: front-illuminated charge-coupled device (FI CCD) cameras, where light is incident on an electrode before reaching the photosensitive silicon layer, and back-illuminated charge-coupled device (BI CCD) cameras, where the incoming light falls directly on the silicon layer (Figure 3.12). Note that the structure of an FI CCD is similar to the anatomy of the human eye. In the retina, it is the nerve "wiring" that faces the incoming light. Only after light has passed the layer of nerve cells that are not sensitive to light can the photons interact with rhodopsin in the photoreceptors.

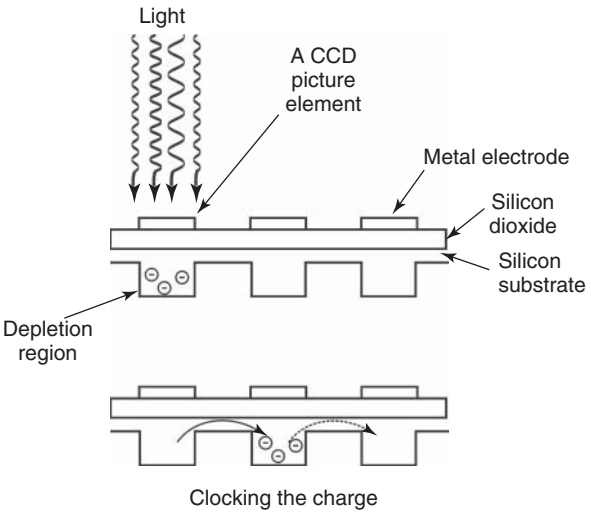

Figure 3.11 Converting photons into electric charges and their transfer in a CCD array.

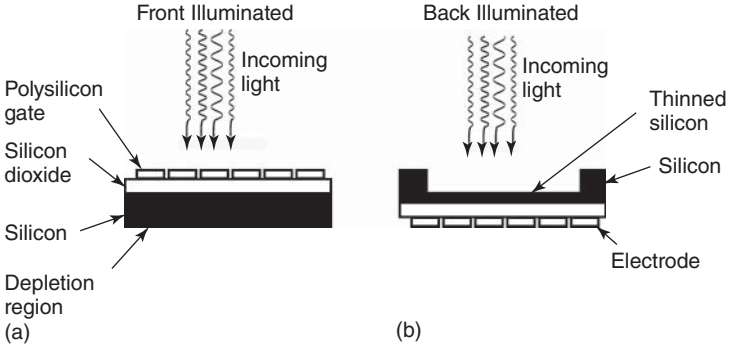

Figure 3.12 Architecture of a (a) front- and (b) back-illuminated CCD.

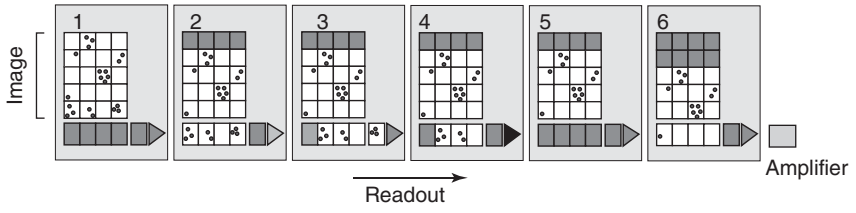

Figure 3.13 Charge transfer through a CCD array and into an amplifier.

When the array of light-sensitive elements (capacitors, photodiodes; in digital microscopy called *picture elements* or *pixels* for short) of a camera is exposed to light, each of them accumulates an electric charge (Figure 3.11). These charges are later read one by one. An electronic control system shifts each charge to a neighboring element, and the process is repeated until all charges are shifted to an amplifier (Figure 3.13). When the individual charges are dumped onto a charge amplifier, they are converted into corresponding voltage values. This process is

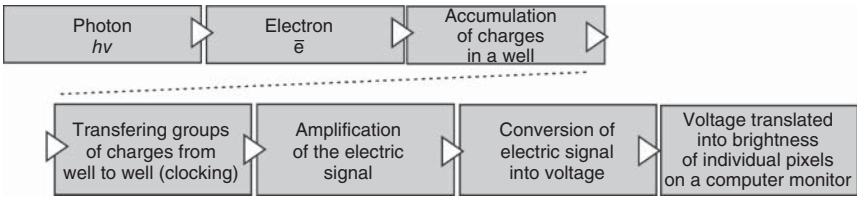

Figure 3.14 A schematic representation of the steps occurring from the absorption of a photon in a CCD array to the display of brightness on a computer screen. In some digital cameras, amplification of the signal is achieved already on the chip (see sections below).

repeated until all the light detected by a microscope in all pixels of the field of view is eventually translated, point by point, into voltage values. The values of these voltages are subsequently converted into discrete values (digitized) and translated into the levels of brightness (intensity of light) on the display screen (Figure 3.14). Sensitivity of a CCD camera and its ability to record strong signals depend on a number of factors, including the level of electronic noise and the ability to accumulate a large number of charges. Weak signals may be undetectable if they are comparable to the noise level. Strong signals may also be difficult to record faithfully. Exposing a CCD array to a large dose of light may result in filling the well with charges and reaching the maximum well capacity (saturation charge). This may cause charges spilling into the neighboring wells and result in deterioration of image quality.

In an ideal situation, only the photons that strike the silicone surface of a light-sensitive element of the camera should actually cause accumulation of an electric charge, which is later shifted and read out (Figure 3.14). However, some electrons may occur and be recorded even in the absence of any incident light. This contributes to the noise of the displayed image (see below). As fluorescence intensities encountered in microscopy are usually low, the fluorescence signal may be difficult to detect in the presence of substantial camera noise (for a comprehensive discussion of camera noise, see Section 12.3.3). In order to alleviate this problem, photons registered by the neighboring elements of an array can be combined and read as one entity. This procedure, called *binning*, is illustrated in Figure 3.15. A fluorescent structure in a specimen is symbolized by two black lines. It is overlaid with a fragment of a CCD array. The weak signals recorded in individual small pixels of a 6×6 array do not stand out well against the background noise generated by the electronics of the camera. When a 3×3 array of larger pixels is used, signals from the areas corresponding to four neighboring small pixels are summed up. Such signals become sufficiently strong to be detected well above the noise floor. The improvement in signal-to-noise ratio is achieved at the cost of spatial resolution. Note that Figure 3.15 is intended to explain the principle and benefit of binning, but it is a necessary oversimplification because it does not consider the dark noise generated in each pixel by thermal noise in the device; this noise will also be summed in the binning procedure.

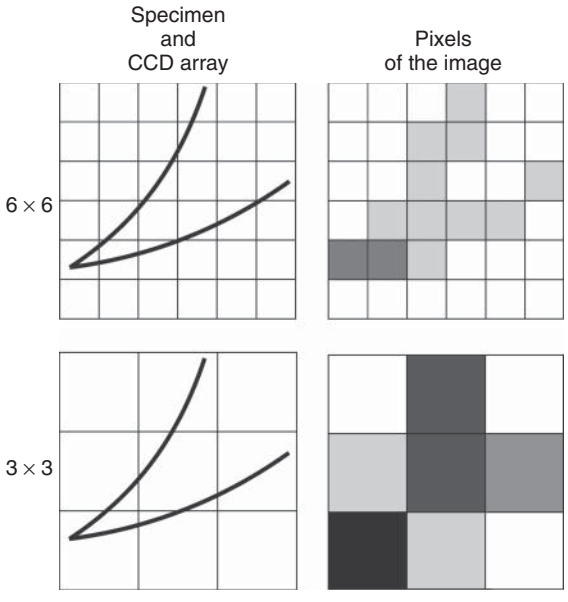

Figure 3.15 A schematic diagram describing the principle of binning in a CCD sensor.

Longer recording times also help to isolate weak signals from random noise. Weak fluorescence signals that are below the detection level of a standard CCD camera may be detected by ICCD and EMCCD cameras (see below).

The light-sensitive element of a CCD camera cannot detect all incident photons because not all photons that arrive at a given pixel generate an electron. The ratio between the incident photons that generate an electric charge to all photons incident on an area of a detector is referred to as the *quantum efficiency* of a CCD camera. This efficiency is wavelength-dependent. FI CCD cameras reach 60–70% quantum efficiency in the visible range and are essentially unable to detect UV radiation (Figure 3.16). BI CCDs have a quantum efficiency (QE) of up to 95% and a better spectral response, including the ability to detect in the UV range. The difference arises from the fact that the BI CCD exposes light-sensitive elements, rather than an electrode structure, as in FI CCD, directly to the incoming light.

3.4.7 Intensified CCD (ICCD)

Fluorescence microscopy invariably struggles with weak signals. Image acquisition is particularly difficult when a high speed of data recording is required. A standard CCD camera is often insufficient for the detection of faint fluorescence due to a high readout noise. Moreover, high sensitivity of a standard CCD sensor is achieved only at relatively low image acquisition rates. Much better sensitivity is offered by an ICCD camera. While a standard CCD-based camera produces only one electron in response to one incoming photon, an ICCD generates thousands of electrons.

ICCDs use an amplifying device called a *microchannel plate*, which is placed in front of a standard CCD light sensor (Figure 3.17). A microchannel plate consists

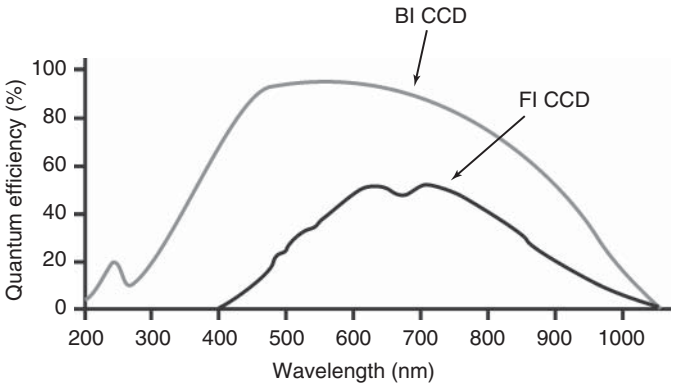

Figure 3.16 Quantum efficiency and spectral response of front- and back-illuminated CCDs. (Documentation from Andor Company, simplified.)

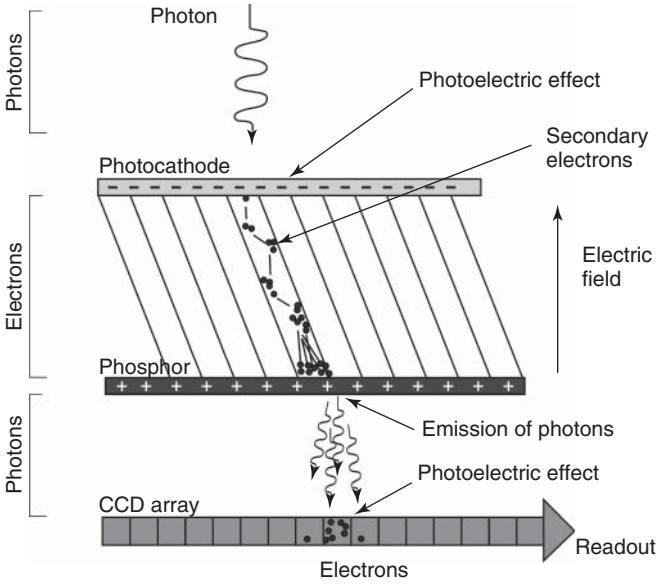

Figure 3.17 Signal amplification in an intensified CCD sensor.

of a photocathode, a set of channels, and the layer of a phosphor. A photon incident on a photocathode generates one electron (by means of the photoelectric effect) that travels inside a channel, toward the phosphor layer, and is accelerated by a strong electric field. Inside the channel, the electron hits the channel walls and generates more electrons that eventually reach the phosphor. There, each electron causes the emission of a photon which is subsequently registered by the sensor of a standard CCD camera. In this way, the microchannel plate amplifies the original weak light signal, and this amplified signal is eventually detected by a standard CCD sensor. In ICCDs, the signal-to-noise ratio can be improved by a factor of several thousand in comparison with a standard CCD camera.

ICCD cameras feature the high sensitivity that is required for the imaging of weak fluorescence signals (although the sensitivity of the primary photocathode is relatively low, not exceeding 50% quantum efficiency). However, the spatial resolution is low and background noise is usually high. Moreover, an ICCD chip can be damaged by excess light. When a high data registration speed is needed and the signal is weak, an EMCCD camera is a viable option.

3.4.8 Electron-Multiplying Charge-Coupled Device (EMCCD)

Another option available for detection of weak fluorescence signals is an EMCCD camera. This device is characterized by a very low read noise and offers sufficient sensitivity to detect single photons. It features high speed, high quantum efficiency, and high digital resolution. In this type of camera, amplification of the charge signal occurs before the charge amplification is performed by the electron-multiplying structure built into the chip (hence called *on-chip multiplication*).

An EMCCD camera is based on the so-called frame-transfer CCD (Figure 3.18; this technology is also used in some conventional CCDs) and includes a serial (readout) register and a multiplication register. The frame-transfer architecture is based on two sensor areas – the area that captures the image, and the storage area where the image is stored before it is read out. The storage area is covered with an opaque mask. The image captured by the sensor area is shifted to the storage area after a predefined image integration time, and subsequently read out. At the same time, the next image is acquired. The charge is shifted out through the readout register and through the multiplication register where amplification occurs prior to readout by the charge amplifier. The readout register is a type of a standard CCD serial register. Charges are subsequently shifted to the multiplication register, that is, an area where electrons are shifted from one element to the next one by applying a voltage that is higher than typically used in a standard CCD serial register. At an electric field of such a high value, the so-called secondary electrons are generated. The physical process that is activated by this voltage is called *impact ionization*. More and more electrons enter subsequent elements of the multiplication register, and a "snowball effect" ensues: the higher the voltage (for an operator – the *gain* value) and the larger the number of pixels in the multiplication register, the higher the overall multiplication of the original faint fluorescence signal (Figure 3.18). The process of multiplication is very fast, so an EMCCD camera is not only very sensitive but also very fast while preserving the high spatial resolution of a standard CCD chip.

The probability of generating a secondary electron depends on the voltage of the multiplication clock (Figure 3.19a) and the temperature of the sensor (Figure 3.19b). Although the efficiency of generating a secondary electron is quite low (~0.01 per shift), this process can occur in all elements of a long multiplication register, bringing the final multiplication value to several hundred or more. But this amplification is not for free. As the generation of the electrons is a stochastic process in each pixel, the extra gain increases the noise in the

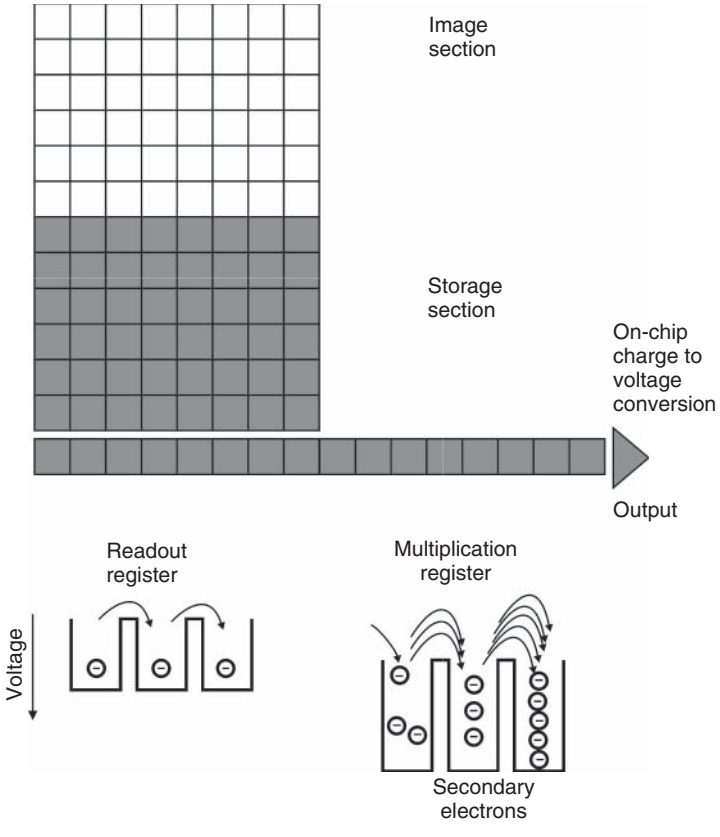

Figure 3.18 Principle of operation and signal amplification in an EMCCD sensor.

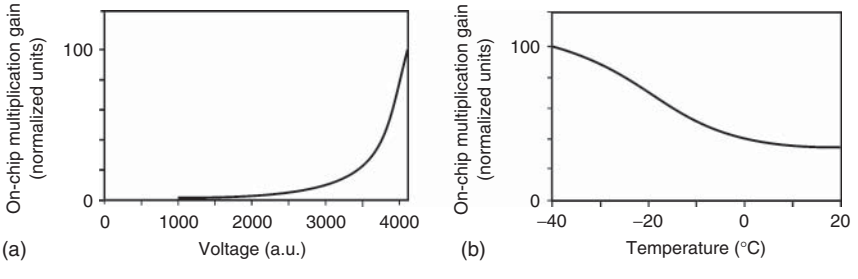

Figure 3.19 On-chip multiplication gain versus (a) voltage and (b) temperature in an EMCCD camera. (Source: Roper Scientific Technical Note #14.)

signal. This is accounted for by the so-called noise excess factor, F (see also Section 12.3.3).

The probability of generating a secondary electron decreases with temperature, as shown in Figure 3.19. Thus, cooling a chip gives an additional advantage in terms of a higher on-chip multiplication gain. Cooling a chip from room temperature to −20 °C increases the chance of generating a secondary electron by

a factor of 2. Some EMCCD cameras are cooled to −100 °C. The lower temperature also results in a lower dark current (see below). Thus, even a very weak signal becomes detectable because it stands out above the noise floor. Reducing the noise level at low temperatures is particularly important because all signals that occur in a well or a serial register, and do not represent the fluorescence signal, will be multiplied with the signal of interest.

3.4.9 CMOS

An alternative to a CCD is a complementary metal–oxide–semiconductor (CMOS) image sensor. Note that the term CMOS actually refers to the technology of manufacturing transistors on a silicone wafer, not the method of image capture. Like the CCD, CMOS exploits the photoelectric effect. Photons interacting with a silicon semiconductor move electrons from the valence band into the conduction band. The electrons are collected in a potential well and are converted into a voltage that is different from that in a CCD sensor, where the charge is first moved into a register and subsequently converted into voltage. The measured voltage is then passed through an analog-to-digital converter and translated into a brightness value for an individual pixel on the computer monitor. CMOS sensors are manufactured in a process where the digital logic circuits, clock drivers, counters, and analog-to-digital converters are placed on the same silicon foundation and at the same time as the photodiode array. In this respect, the architecture of a CMOS sensor is distinctly different from that of a CCD device, where the charge of each photodiode is transferred first to the chip, and then read out in sequence outside of the chip.

The construction of a typical CMOS photodiode is presented in Figure 3.20. The actual light-sensitive element and the readout amplifier are combined into

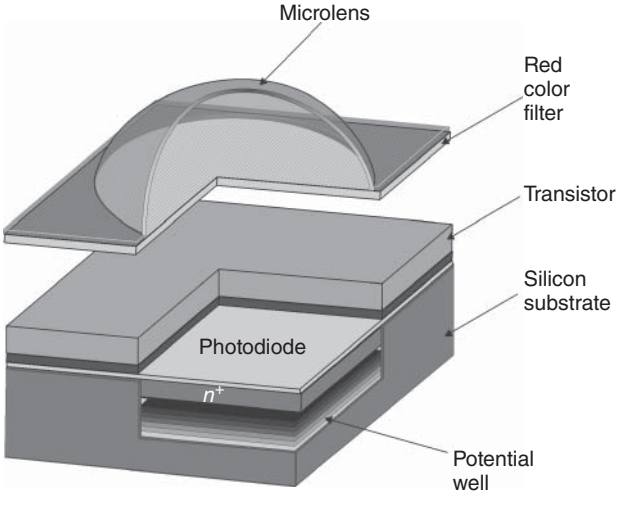

Figure 3.20 Architecture of a single CMOS photodiode. (A figure by M. Davidson, Microscopy Primer, University of Florida, modified.)

one entity. The charge accumulated by the photodiode is converted into an amplified voltage inside the pixel and subsequently transferred individually into the analog signal-processing portion of the chip. A large part of the array consists of electronic components, which do not collect light and are thus not involved in detecting the light incident on the sensor. The architecture of the array leaves only a part of the sensor available for light collection and imposes a limit on the light sensitivity of the device. This shortcoming is minimized by placing an array of microlenses over the sensor, which focus the incident light onto each photodiode.

The unique architecture of a CMOS image sensor makes it possible to read individual pixel data throughout the entire photodiode array. Thus, only a selected area of the sensor can be used to build an image (window-of-interest readout). This capability makes CMOS sensors attractive for many microscopy applications. CMOS technology has been refined in recent years so that today's sensors compete successfully even with high-end EMCCD cameras in many low-light microscopy applications. At the time of writing, 2048×2048 pixel CMOS sensors using 6.5×6.5 µm pixels with a quantum efficiency exceeding 70% and a 100 frames per second readout rate are available.

3.4.10 Scientific CMOS (sCMOS)

CMOS-based digital cameras were originally inferior to high-end CCD cameras. Until recently, EMCCD cameras were the best choice in terms of sensitivity, speed of data acquisition, and digital resolution. Yet the CMOS technology has made significant advances, and the newest design, called scientific CMOS (sCMOS), is challenging even the EMCCD sensors in many demanding microscopy applications. The advantages of the sCMOS sensor include a large-size array, small pixel size, low read noise, high frame rate, high dynamic range, and no multiplicative noise.

3.4.11 Features of CCD and CMOS Cameras

CMOS and CCD cameras are inherently monochromatic devices, responding only to the total number of electrons accumulated in the photodiodes and not to the color of light that gives rise to their release from the silicon substrate. In fluorescence microscopy, detection of two or more colors is often required. Sets of emission optical filters are then used to collect images in selected spectral bands sequentially. When simultaneous measurements are necessary, two digital cameras are mounted on a microscope stand.

Although the same type of CCD chip is used by many manufacturers of digital cameras, the ultimate noise level, speed of data acquisition, and dynamic range of a given camera may be quite different. These differences arise from the differences in electronics and software driving the camera. The user should explore the features and software options of the camera to identify the sources of noise, to calibrate the camera, and to optimize image collection for the specific type of experiment.

3.4.12 Choosing a Digital Camera for Fluorescence Microscopy

It might seem obvious that a researcher who is planning to purchase a new fluorescence microscopy system should buy, funds permitting, the best digital camera on the market. However, there is no "best digital camera" for fluorescence microscopy as such. The camera should be selected for a given application. Manufacturers provide important information about the chip and the software, including the pixel size, quantum efficiency, full well capacity, the size of the various noise contributions, speed of image acquisition and the corresponding achievable resolution, tools for calibration, and noise removal, and so on. Careful analysis of technical parameters of various cameras available on the market is essential. However, nothing can substitute testing the various cameras with a typical specimen, which is the researcher's prime object of investigation.

3.4.13 Photomultiplier Tube (PMT)

While the CCD and CMOS cameras briefly introduced above are used for recording the whole image of a field of view essentially at the same time in a parallel process, a photomultiplier is used as a point detector. In other words, it records the intensity of light only in one selected point of the image at a time. Thus, photomultiplier tubes (PMTs) are not used in standard widefield fluorescence microscopes, but serve as light detectors in laser scanning confocal microscopes.

A PMT is a signal-amplifying device that exploits the photoelectric effect and a secondary emission phenomenon, that is, the ability of electrons to cause the emission of other (secondary) electrons from an electrode in a vacuum tube. Light enters a PMT through a quartz (or glass) window and strikes a photosensitive surface (a photocathode) made of alkali metals (Figure 3.21). The photocathode releases electrons that subsequently strike the electrode (dynode), which releases a still larger number of electrons. These electrons hit the next dynode. A high voltage (1–2 kV) is applied between subsequent dynodes.

The electrons are accelerated and the process is repeated, leading to an amplification of the first electric current generated on the photocathode. The current

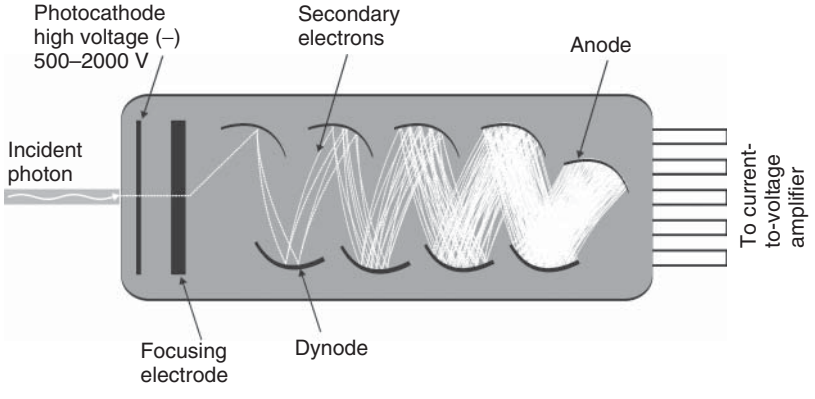

Figure 3.21 Schematic of a photomultiplier.

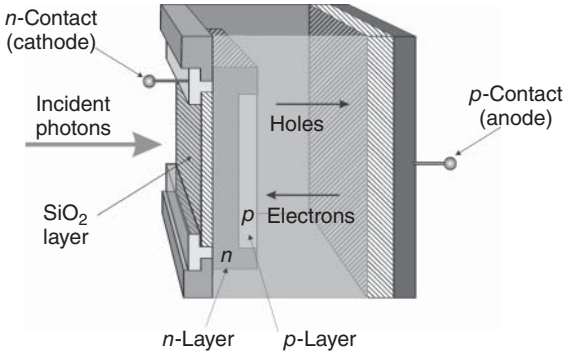

Figure 3.22 Schematic of an avalanche photodiode. (A figure by M. Davidson, Microscopy Primer, University of Florida, modified.)

measured at the last dynode is proportional to the intensity of light that was incident on the photocathode. The gain obtained by amplifying the electric current through subsequent dynodes can be as high as 10^7–10^8. However, the voltage that is applied to the dynodes causes a low-level electron flow through the PMT even in the absence of light. This is translated into a non-zero-level reading on a fluorescence image. The quantum efficiency of a PMT does not exceed 30%. PMTs are very fast detectors of UV and visible light. They can be used to detect single photons and follow extremely fast processes, as the response time can be as low as several nanoseconds. Typically, in laser scanning confocal microscopes, sets of 2–5 PMTs are used as fluorescence detectors in selected wavelength bands.

3.4.14 Avalanche Photodiode (APD)

An APD is also a signal-amplifying device that exploits the inner photoelectric effect. A photodiode is essentially a semiconductor p–n (or p–i–n) junction (Figure 3.22). When a photon of sufficient energy strikes the diode, it excites an electron, thereby creating a free electron (and a positively charged electron hole). This, in turn, creates a flow of electrons ("an avalanche") between the anode and the cathode, and electron holes between the cathode and the anode, because a high voltage is applied between the anode and the cathode. Electrons accelerated in the electric field collide with atoms in the crystalline silicon and induce more electron–hole pairs. This phenomenon amounts to a multiplication effect. In this respect, an APD bears similarity to a PMT. The quantum yield of an APD can reach 90%, that is, it is substantially higher than that of a PMT, and the response time is several times shorter. However, the gain is lower, in the range of 500–1000. Single-photon avalanche photodiodes (SPADs) are currently used as detectors in fluorescence lifetime imaging microscopy (FLIM).

3.5 Types of Noise in a Digital Microscopy Image

If a light detector were ideal, an image collected in the absence of any specimen should be completely black. However, even in the absence of any fluorescence in the sample, CCD sensors still generate certain readout values that are greater than

zero. In laboratory vocabulary, these weak unwanted signals that do not represent fluorescence are generally called *background* or *noise*.

The adverse influence of noise on the quality of the recorded image is understandable. Let us assume that the noise signals have a value in the range between 1 and 10 on a scale of 1–100. If a signal representing fluorescence has an intensity of 80, it will be readily detected, but if a weak signal has an intensity of 10, it will not be distinguishable from the noise (Figure 3.23). Averaging a large number of image frames should make the signal detectable over the noise level, but an experimenter rarely has the luxury of collecting many images of the same field of view because photobleaching will inevitably diminish the fluorescence signal, while the noise level will remain the same. The range of intensities of fluorescence signals that can eventually be recorded above the level of noise is called the *dynamic range of the detector*. More precisely, dynamic range is the ratio between the maximum and the minimum level of signal that can be detected. Thus, the dynamic range of a CCD camera is equal to the saturation charge (full well capacity) divided by the readout noise (i.e., the noise generated in the absence of light), when both are expressed as the number of electrons. A higher dynamic range of a camera means a broader range of fluorescence intensities that can be faithfully recorded (Figure 3.24). It should be noted, however, that the dynamic range of a light detector defined that way does not provide any information about its absolute sensitivity.

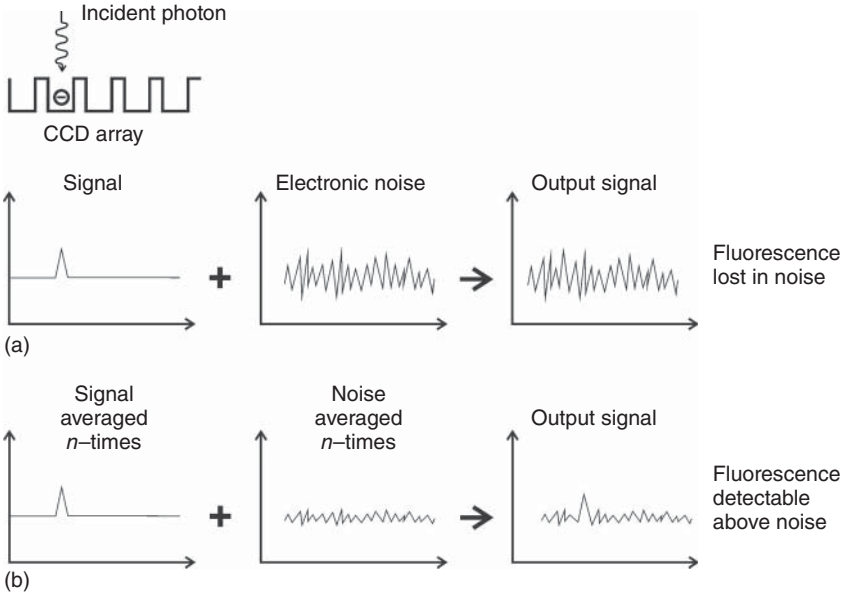

Figure 3.23 Signal averaging and detection of weak fluorescence signals. (a) A weak signal cannot be detected if it is comparable with the level of noise generated by the electronics of a camera. (b) When images of stable fluorescence signals are averaged, the noise is averaged out and becomes relatively low in comparison with the signal. This simplified scheme does not take dark noise into account.

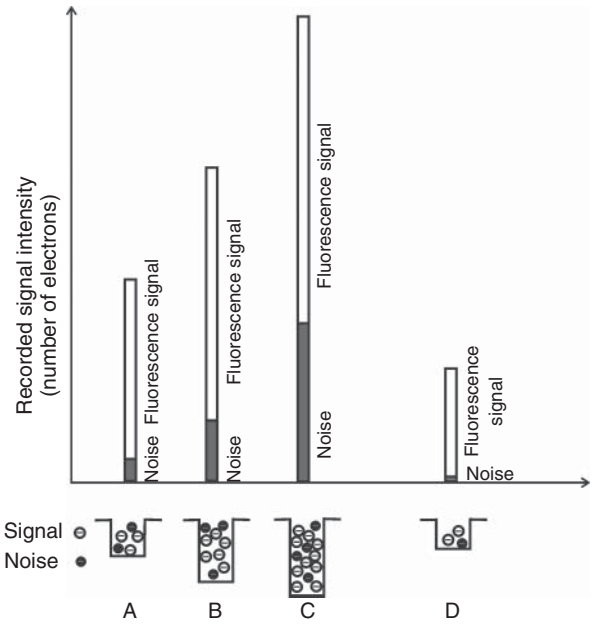

Figure 3.24 A schematic representation of dynamic ranges and sensitivities of four hypothetical digital cameras. The input signals received by cameras A, B, C, and D are such as to fill the charge wells; thus they are different in each case. The recorded signals consist of a noise contribution and fluorescence photons, as shown schematically by the bars. The electrons resulting from noise and fluorescence that fill the wells to a maximum capacity are shown symbolically below the bars. Cameras A, B, C, and D generate different levels of noise; therefore, their ability to detect weak signals differs. Sensors A, B, and C have similar dynamic ranges, that is, the ratio between the maximum recordable fluorescence signal and the level of noise is similar, but the ability to detect the strong signals differs – it is the best for camera C. Camera A is more sensitive than camera B or C. Camera D has a very low dynamic range but it has a very low noise level; thus, it is the most sensitive of the four. Camera D is not suitable for detecting strong signals. Different levels of the maximum recordable signal of these cameras are a consequence of different well depths of their sensors.

A weak fluorescence signal can be "fished out" of the noise by increasing the integration time (Figure 3.25). This simple procedure will be useful only if the rate of photobleaching does not offset the benefit of integration. Integration takes considerable time. Therefore, although weak signals can eventually be recorded by a CCD camera, the process may be relatively slow.

Another way to detect a weak signal is to use an ICCD or an EMCCD. These devices use two different ways of amplification of the signal before it is actually read out, that is, before an unavoidable addition of the read noise takes place. In order to fully appreciate different strategies that were used by digital camera developers aiming at enabling detection of weak signals, a brief discussion of various types of noise is required.

Some sources of noise were mentioned when speaking about the principles behind and construction of various camera types. Generally, one can identify

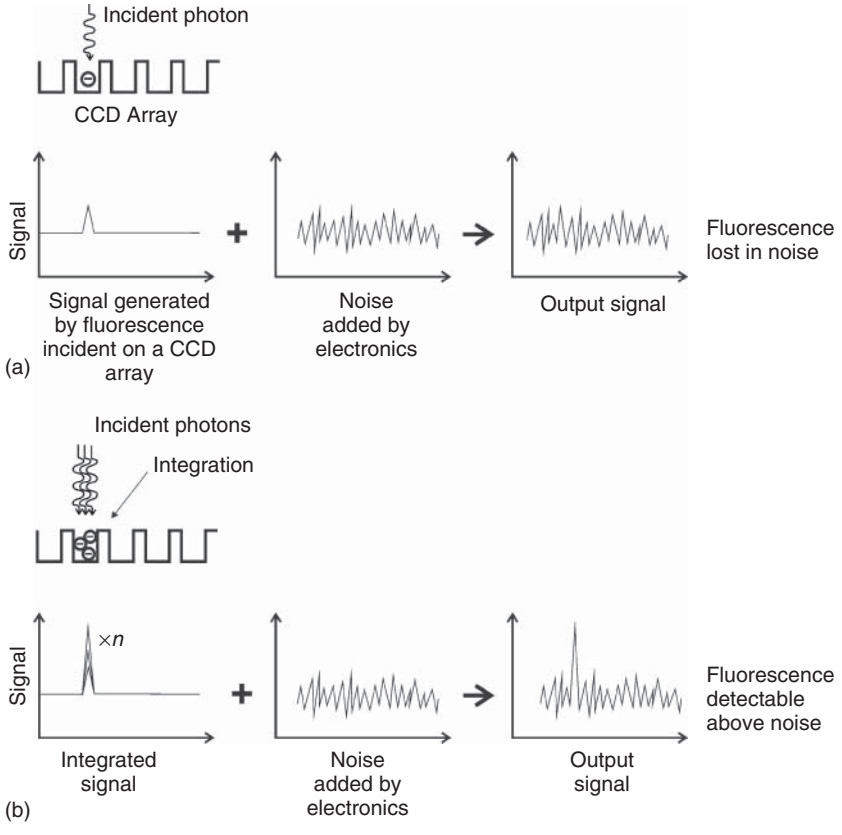

Figure 3.25 Integration elevates weak signals above the noise level. Integration, which is the summing up of incident fluorescence photons, improves the signal-to-noise ratio because the level of electronic noise added after signal integration remains constant. This simplified diagram does not take dark noise into account. (a) Signal collected as one frame, that is, without integration. (b) Integration of signals.

three major sources of noise in a digital microscopy image registered by a camera: (i) dark current noise, (ii) photon noise, and (iii) read noise.

The *dark current* (dark noise) arises from electrons that are generated in a well of a semiconductor sensor in the absence of any external light as a result of electron emission due to thermal motion. When the integration time on the CCD chip is increased, the accumulating thermal charge also increases. This leads to a detectable background in the image. As the electron emission is dependent on temperature, cooling the camera chip efficiently reduces the dark current. The dark current can be decreased from the final image by subtraction. Dark current noise should not be confused with background signal arising from low-level autofluorescence or fluorescence arising from nonspecific binding of an antibody in an immunofluorescence preparation.

The *photon noise* or *shot noise* results from the quantum nature of light. It is a term that refers to the temporal distribution of photons arriving at the surface of

a sensor. Even if the fluorescence-emitting object is flat and uniformly stained, the frequency of photons arriving at the light-sensitive element of the sensor is governed by chance. The frequency of photon arrival follows the so-called Poisson statistics. This implies that the number of photons originating in a given small volume of a continuously illuminated specimen and subsequently reaching the detector varies in different time intervals (we ignore photobleaching for simplicity). This also implies that when the same (nonbleaching) voxel in the specimen is imaged repeatedly, and in a given measurement the number of detected photons is n, the subsequent determinations of the number of photons vary within a range of $\sqrt{n}$. Shot noise can be quite misleading. Inexperienced microscopists often take the grainy structure of an area in the image for a real variation of the fluorescence signal, or interpret differences between local signal intensities as evidence for a difference in the concentration of a fluorescent label. However, such features of the image may merely be a consequence of a very low number of photons that are typically collected in fluorescence microscopy studies.

The *read noise* arises in the process of converting a charge generated in the sensor well into voltage and digitization. Camera manufacturers provide information about the noise generated "on-chip" by specifying a root-mean-square (RMS) number of electrons per pixel. For instance, $10\,e^-$ RMS means that a read noise level of 10 electrons per pixel is expected. Thus, the signal obtained after readout of the charges would show a standard deviation of 10 electrons, even if all pixels contained identical numbers of electrons. At low signal levels, photon noise is the most significant noise contribution. As vendors may interface the same type of a light-sensitive chip with different electronics, the levels of electronic noise in cameras from different sources may also be different.

In addition to the major sources of noise mentioned above, other factors may result in unpredictable signal variability or nonzero levels. These factors include the nonuniformity of photoresponse, that is, noise values dependent on the location in the image sensor, and the nonuniformity of dark current. Nonuniformity of photoresponse is a consequence of the fact that individual pixels in a CCD chip do not convert photons to electrons with identical efficiency. Pixel-to-pixel variation is usually low in scientific-grade cameras and generally does not exceed 2%. The correction for differences between light sensitivity of individual pixels can be achieved by recording an image of an ideally uniform fluorescent object, for instance, a dye solution, and creating a correction mask using standard image processing tools. Dark current nonuniformity results from the fact that each pixel generates a dark current at a slightly different rate. The dark current may also drift over a longer period, for instance, owing to a change in the sensor's temperature.

In summary, different types of noise contribute differently to the final image. On-chip multiplication represented by ICCD, CMOS, and EMCCD digital cameras has opened new avenues of research by making it possible to detect very weak signals quickly and with a high spatial resolution.

3.6 Quantitative Fluorescence Microscopy

3.6.1 Measurements of Fluorescence Intensity and Concentration of the Labeled Target

A fluorescence microscopy image is usually treated as a source of information about structure, that is, about the spatial distribution of a molecule of interest. Let us use an immunofluorescently stained image of microtubules in a fibroblast as an example. On the basis of such an image, the observer can establish the presence or absence of tubulin in a given location of a cell. The local intensity of the fluorescence signal is not used here as a source of information about the local concentration of tubulin. Such information is not available because the strength of the fluorescence signal depends on the location of the microtubule in relation to the plane of focus. Using the fluorescence signal as a source of information about the local concentration of tubulin is also impossible because immunofluorescence staining may be nonuniform, as the antibody may be sterically hindered by other proteins from accessing the microtubule. Thus, in this example, the only information required and expected is the architecture of a network of microtubules. The interpretation of the image is based on the assumption that all microtubules stain with an antibody to a degree that makes them detectable.

Often, not just the presence or absence, but also the local *concentration* of the labeled protein or other molecular target is of interest. Extracting this information requires using a fluorescence microscope as an analytical device. In all honesty, however, one has to admit that a standard widefield fluorescence microscope is not made to be an analytical device capable of straightforward measurements of the quantities of fluorescently labeled molecules within a specimen. This task can be performed more adequately by confocal microscopes. A rough estimate of local concentrations can be made in a widefield fluorescence microscope; however, a microscopist should keep the following considerations in mind.

Any attempt to estimate *relative* (within the same field of view) or absolute concentrations (see below) of fluorescent molecules is based on the tacit assumption that the amount of the bound fluorescent probe is proportional to the amount of molecules of interest. This assumption is rarely true. Let us take DNA-binding fluorescent probes as an example. Among some 50 fluorescent probes that bind DNA, only a few bind it in an (almost) stoichiometric manner (4′,6-diamidino-2-phenylindole (DAPI), Hoechst, propidium, DRAQ5). Most DNA dyes also bind RNA, thus RNA has to be hydrolyzed before measuring the local concentration of DNA. Hoechst and DAPI have low affinity for RNA, but propidium is an example of a probe with high affinity for RNA. Nevertheless, propidium is a popular DNA probe used for measuring DNA content in cells by flow and laser scanning cytometry. Measurement of the absolute DNA amounts is also complicated by the fact that propidium as well as other DNA-affine dyes compete with proteins for binding to DNA. It has been demonstrated that the amount of propidium bound to DNA is higher in fixed cells, following removal of some of the DNA-associated proteins. This means that assessment of DNA

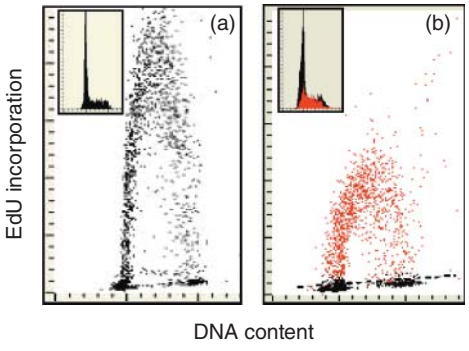

Figure 3.26 Laser scanning cytometry (LSC) determination of DNA content per cell, and the amount of newly synthesized DNA per cell (after delivering a pulse of DNA precursor, EdU; see also Figure 3.4) in a large population of cells. DNA was stained by DAPI; EdU was fluorescently labeled with AlexaFluor 488. (a) Untreated control culture and (b) cells exposed to hydrogen peroxide (200 μM) for 60 min, showing a reduced amount of nascent DNA. EdU-incorporating cells are marked with red and are shown in a DNA histogram in the inset. Each dot plot or histogram represents blue (DAPI) and green (EdU) fluorescence signals measured in over 3000 cells. The insets in (a) and (b) show DNA frequency histograms, based on DAPI signals from the respective cultures. (Zhao et al. [22].)

content requires careful calibration within the investigated system, including using the same type of cells, the same procedure of RNA removal, and so on. When these measures are taken, the assessment of the local concentration of DNA can be quite precise. Simple and reliable determinations of relative amounts of DNA in individual cells can be achieved by staining DNA with DAPI or Hoechst and recording images with a laser scanning cytometer (LSC, Figure 3.26).

Measurements of the *absolute* concentrations of a fluorescently labeled target are more difficult than measurements of relative concentrations within the same field of view. When attempting such measurements, a microscopist needs to consider the limitations described in the previous sections and the following factors that influence the estimate:

- linearity of the detector response;
- dynamic range of the detector;
- vignetting, that is, fluorescence intensity being lower at the edges than in the image center;
- light collecting efficiency and transmission of different objective lenses;
- the influence of the position of the focal plane in relation to the object;
- nonuniform bleaching of the fluorescent probe in different cellular compartments;
- dynamic exchange of the fluorescent probe that occurs in the case of equilibrium staining;
- the influence of collisional quenching of fluorescence (probe to probe or probe to oxygen);
- possible increase of fluorescence intensity resulting from bleaching of self-quenching probes;

- changes in the spectral properties of fluorescent probes upon exposure to exciting light;
- the inner filter effect.

Even this long list of factors may turn out not to be exhaustive in the case of some fluorescent probes and types of samples. It certainly illustrates the fact that measuring the concentrations of fluorescently labeled molecules in microscopy is a cumbersome task, to say the least.

There is at least one important example of relatively accurate measurements of absolute intracellular concentrations in fluorescence microscopy. These are the so-called ratio measurements of calcium and other ions in live cells. They are described briefly in the following section.

3.6.2 Ratiometric Measurements (Ca^{++}, pH)

Some fluorescent dyes respond to changes in calcium or hydrogen ion concentration not just by changing the intensity of fluorescence but by changing the spectral properties of two emission bands (Figure 3.27). In this case, a ratio, but not the absolute fluorescence intensity, can be linked to the calcium concentration or pH value. This approach has a very important advantage. In principle, the ratio between these two emissions is independent of the local concentration of the fluorescent probe. Thus, typically encountered changes of the dye concentration arising from influx, pumping out by multidrug resistance (MDR) mechanisms, photobleaching, and so on, should not influence the measurement. A detailed discussion of the advantages and limitations of ratiometric studies of intracellular calcium and pH goes far beyond the scope of this book. The reader is advised to also consider the limitations of these techniques, arising from the fact that the calcium dyes chelate these ions and thus may disturb the intracellular calcium balance and the fact that exposing intracellular calcium indicators to light is likely to generate singlet oxygen and cause various phototoxic effects [7]. A careful calibration and optimization of ratiometric studies is required.

3.6.3 Measurements of Dimensions in 3D Fluorescence Microscopy

Calibration and measurement of dimensions in the plane of the specimen is straightforward, as described in basic microscopy books. Modern widefield fluorescence microscopy, including microscopy with image deconvolution, deals with 3D rather than 2D objects, so accurate measurements of dimensions along the optical axis are important as well. This measurement is somewhat more complicated because a movement of the objective in relation to the specimen by a given distance does not necessarily shift the image plane by the same distance within the studied specimen. A possible difference may arise from the mismatch between the refractive indices of the immersion medium and the sample, and is caused by spherical aberration. This is most pronounced in the case of an oil-immersion objective lens used to image at a distance from the surface of a coverslip deep into a water-containing sample (Figure 2.22). The effect is less pronounced in the case of a water-immersion lens.

It is worth noting that *size* measurements of subcellular objects in fluorescence microscopy are limited by diffraction and dependent on wavelength. In the

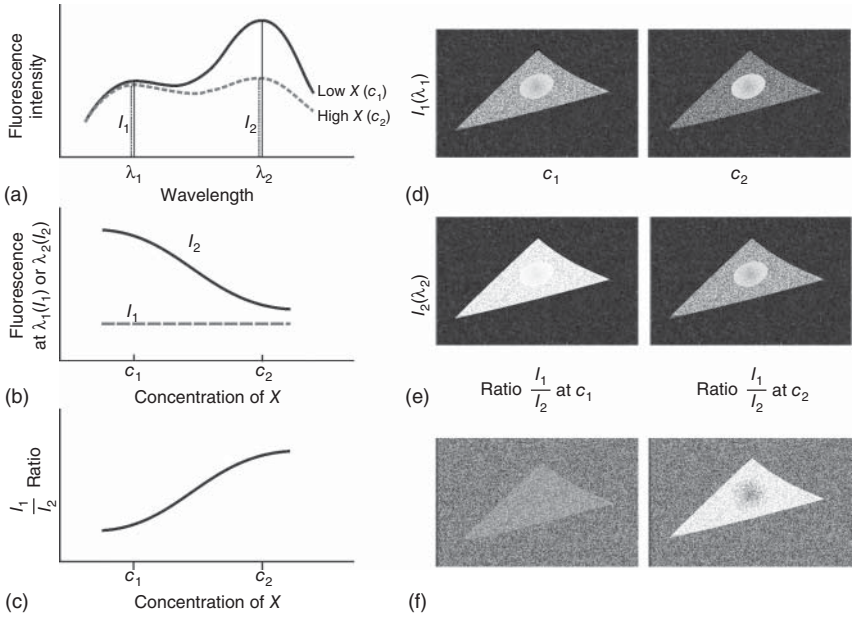

Figure 3.27 The basic principle of fluorescence ratio measurements. The emission spectrum of a fluorophore, shown schematically in (a), is a function of the concentration of a molecule *X* – for instance, calcium ions. At the wavelength λ_1, the emission intensity I_1 is independent of *X*, whereas at λ_2 the emission intensity I_2 decreases with concentration of *X*, as shown in (b). Different intensities of fluorescence of *X* detected at λ_1 within one cell reflect different local concentrations of the probe. At λ_2, intracellular fluorescence intensities are a function of local concentrations of the probe as well as the local concentrations of molecules of *X*. The ratio of the intensity of emission I_1 (at λ_1) and I_2 (at λ_2) can be used as a measure of the concentration of *X*, as shown in (c). A schematic representation of images collected at λ_1 and λ_2 at two different concentrations of $X(c_1, c_2)$ is shown in (d, e), and "ratio images" are shown in (f). In these images, each pixel depicts a ratio between values of I_1 over I_2. This value is independent of the local concentration of the probe and reveals a concentration of *X* in the cell. (Adapted from Dobrucki (2004), with kind permission of Elsevier)

plane of the specimen, dimensions of the object smaller than half a wavelength cannot be determined. Object length measurements along the optical axis are approximately 3 times less accurate. However, the *distances* between subresolution objects can be measured much more precisely. For instance, the distances between the barycenters of various small subcellular objects have been measured successfully in various microscopy experiments. Fluorescence microscopy also has another sophisticated tool to detect molecules that are less than a few nanometers apart. This approach is based on fluorescence resonance energy transfer (Chapter 13).

3.6.4 Measurements of Exciting Light Intensity

It is often necessary to know and compare the intensity of exciting light emerging out of the objective lens. Such measurements may be needed to calibrate the system in quantitative microscopy or to check the alignment of optical components.

Power meters that are calibrated for measurements of light intensities of various wavelengths are available. A note of caution is needed here because such meters typically have a flat entry window that is to be placed against the incoming light. The high-NA (numerical aperture) oil- and water-immersion lenses produce a cone of light that cannot be measured accurately by such power meters. The outermost light rays hit the meter's window at an angle, which results in reflection. Consequently, a simple flat-window meter placed in front of the high-NA objective lens cannot measure the intensity of the emerging light. Such measurements can be done, for example, for a 10× lens with a low NA.

3.6.5 Technical Tips for Quantitative Fluorescence Microscopy

The ability to perform quantitative fluorescence microscopy hinges upon one's capacity to recognize a number of factors that influence the performance of the microscope and the ability to perform measurements. Besides the parameters that were already mentioned (Section 3.4), these include factors relating to the microscope body, spectral properties, and photophysics of the fluorescent probe and the properties of a particular sample.

Critical issues concerning the microscope include the stability of the exciting light source; chromatic and spherical aberration; channel register, that is, a shift between the images of two color channels in the plane of focus arising from nonideal alignment of the microscope's optical components; the bleed-through between detection channels, that is, detection of photons emitted by one fluorophore in more than one detection channel; dependence of resolution on the wavelength of light emitted by the fluorescent label (i.e., lower resolution for red-emitting labels than blue-emitting ones); chromatic shift of some dyes that occurs upon binding to cellular components; mechanical stability of the microscope; and the choice of optimal excitation versus emission bands.

With regard to the fluorescent probe, one must consider its photobleaching kinetics [8–11]; possible collisional quenching between dyes or between dyes and oxygen, and self-quenching; the possible occurrence of FRET when using more than one color, which would result in an unexpected loss of a donor signal; and, finally, the phototoxic effects. Phototoxicity may result in a supposedly extracellular dye getting into damaged cells, lysosomes bursting during illumination, or calcium oscillations occurring as a result of the action induced by the fluorescent probe itself [7].

Finally, each particular sample has its caveats. To these belong existence of autofluorescence in selected spectral regions [11, 12], the consideration of the inner filter effect, scattering of exciting light [13], or sample aging. Also, one must consider the possible existence of different binding sites for specific labels, as has been discussed in the context of the DNA-staining dyes. This problem often occurs in immunolabeling strategies with antibodies, where cross-reactivities often exist.

One should always keep in mind that the microscope produces a 2D image of samples that are actually three dimensional. As the excitation light illuminates a relatively large area of the specimen in the plane of focus, as well as the regions above and below this plane, fluorescence is always excited in a large volume of

the sample. Both the exciting light and the emitted fluorescence are scattered in this region. This causes substantial out-of-focus light, which is detected as background. Discrete fluorescing sample components appear to be surrounded by a "halo" of light, and even the areas between the fluorescing structures of the specimen seem to fluoresce. This blur and background is minimized in a scanning laser confocal microscope (Chapter 5).

3.7 Limitations of Fluorescence Microscopy

The limits of the range of applications of fluorescence microscopy, and its usefulness in studies of live cells, are delineated by three principal issues, namely, photobleaching of fluorescent probes, their toxicity and phototoxicity, and the limited spatial resolution of images.

3.7.1 Photobleaching

Photobleaching is a process of a gradual loss of fluorescence intensity of the specimen arising from interaction between the exciting light and the fluorescent compound. In this process, the fluorescent dye molecules are photochemically destroyed. As this loss of functional dyes occurs during the observation, photobleaching interferes with the collection of high-quality image data. Optimization of image recording parameters, especially the intensity of exciting light, can dramatically reduce the adverse effects of photobleaching (Figure 3.28).

The loss of a dye's fluorescence in a specimen is usually due to photoxidation, which is the oxidation of dye molecules in the presence of light. Photobleaching of fluorescent probes is generally an irreversible process. Other reactions that are

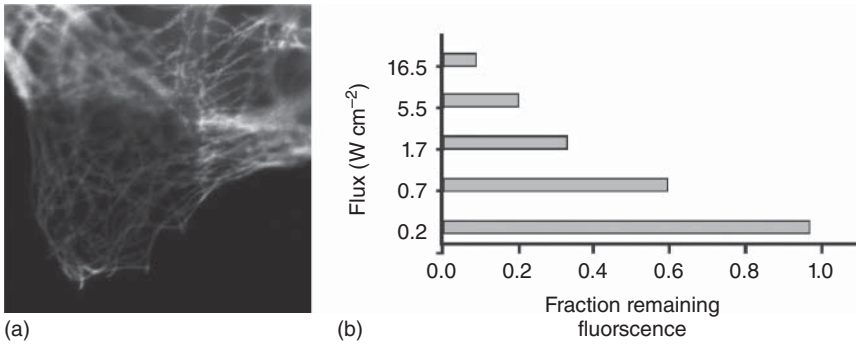

Figure 3.28 Photobleaching. (a) A square area of the fluorescent specimen was exposed to excitation light. The image shows a larger field of view, which embraces the originally illuminated field, thus demonstrating a region that was photobleached. (b) Intensity of exciting light strongly influences rates of photobleaching. In this example, a sample with eGFP was exposed to the same dose of light that was delivered by beams of different intensity. At high light fluxes, fluorescence was bleached almost entirely (only ~10% of the initial signal remained), while using light of almost two orders of magnitude lower intensity necessitated a much longer data collection time but resulted in no detectable loss of signal. Figure from [8]. Reproduced with permission of John Wiley & Sons.

initiated by light and do not involve oxidation but lead to a change of the structure of a fluorescent molecule can also occur.

It is often possible to slow the loss of signal by adding reducing agents and/or scavengers of reactive oxygen species to the sample. These reagents include *N*-propyl gallate and mercaptoethanol. Although homemade or commercial preparations designed to slow down photobleaching can be very effective in preventing signal loss, their addition to the sample often causes a loss of the initial signal's intensity – a phenomenon rarely observed by the microscopist who adds the antioxidant solution to the sample before the first recording of any image [9].

Current applications of photobleaching are a nice example of turning a defeat into victory. Photobleaching, which is such an obstacle to performing successful fluorescence imaging, is exploited today in a number of cutting-edge microscopy techniques such as FRAP and related techniques, detection of FRET by acceptor photobleaching, as well as high-resolution techniques including photoactivation localization microscopy (PALM) [14] and stochastic optical reconstruction microscopy (STORM) [15, 16]. FRAP is based on permanently photobleaching a subpopulation of fluorescent molecules in a selected field of view and recording the rate of return (or lack thereof) of fluorescence due to dynamic exchange of these molecules in the photobleached area (for an extensive discussion, see Chapter 11). PALM, STORM, and related techniques use the ability of some fluorescent molecules to be made transiently nonfluorescent (Chapter 8).

3.7.2 Reversible Photobleaching under Oxidizing or Reducing Conditions

Usually, photobleaching is considered to be an irreversible loss of fluorescence by a fluorophore resulting from exposure to exciting light. As such, photobleaching is one of the main limitations of fluorescence microscopy. It has been discovered, however, that some fluorescent proteins can be reversibly bleached and made fluorescent again by exposure to a different wavelength of light [17]. This property is extremely useful, and is now exploited in modern super-resolution microscopy. Recently, it has been demonstrated that under selected conditions some low molecular weight dyes can also be bleached transiently, meaning that a loss of fluorescence is not permanent and emission can be regained over time or by exposing the sample to intense light of a specific wavelength [18, 19]. Apparently, loss of fluorescence can be made reversible under specific reducing/oxidizing conditions [20].

3.7.3 Phototoxicity

Live cells that are fluorescently labeled and exposed to exciting light are subject to the photodynamic effect. This effect is defined as damage inflicted on cells by light in the presence of a photosensitizer and molecular oxygen. A fluorescent dye that interacts with cell components during a live-cell imaging experiment acts as a photosensitizer and causes various types of damage. The adverse effects caused by low molecular weight dyes usually involve oxygen. Chromophores of fluorescent proteins, such as enhanced green fluorescent protein (eGFP), are shielded by the protein moiety, which prevents direct contact with molecular oxygen. This may explain why fluorescent proteins generally appear to be less phototoxic.

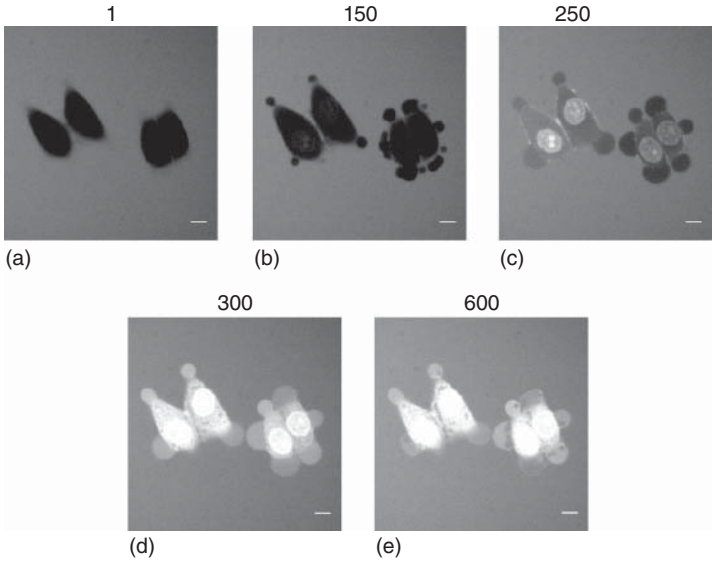

Figure 3.29 An example of phototoxic effects inflicted by a fluorescent probe on live cells. HeLa cells are incubated in culture medium supplemented with ruthenium phenanthroline complex $Ru(phen)_3^{2+}$, which acts as an extracellular photosensitizer (a). The complex is known to generate singlet oxygen when exposed to 458 nm light. Cells cultured on a confocal microscope stage are exposed to 458 nm light (0–600 frames, as indicated above). The first signs of damage are blebbing of the plasma membrane and a slow entry of $Ru(phen)_3^{2+}$ into cell interiors – this is revealed when the complex binds to DNA in nuclei (b, 150 frames). Subsequently, the integrity of plasma membranes is compromised and the complex rapidly enters cells, binds to intracellular structures, and accumulates in cells at a high concentration, which results in bright fluorescence of nuclei and the cytoplasm ((c–e), frames 250–600). (Zarębski et al. [25]).

Phototoxic effects may manifest themselves by readily detectable alterations in cell function, such as a loss of plasma membrane integrity (Figure 3.29), detachment of a cell from the substratum, blebbing, and a loss of mitochondrial potential. However, sometimes even lethal damage can be initially quite inconspicuous. Good examples are the photoxidation of DNA bases, DNA breaks, and so on. Such damage may lead to cell death, but it is not readily detectable during or immediately after a cell imaging experiment. Thus, it is important to recognize that light-induced damage may seriously alter the physiology of the interrogated cell but still remain undetectable for a considerable time. In particular, care is required to establish if the unavoidable phototoxic effects inflicted during a live-cell experiment have sufficient impact on cell physiology so as to influence the interpretation of the collected image data.

3.7.4 Optical Resolution

The Abbe formula (Chapter 2) describes the parameters that influence the optical resolution in the plane of the specimen. However, the formula only applies to images with negligible noise. In fluorescence microscopy, image noise is usually relatively high, while the signals are low and continue to decrease owing to

photobleaching. In fact, under such conditions it is the noise level that becomes the decisive factor defining spatial resolution (Figure 3.30).

The optical resolution of a microscope in the horizontal plane of the specimen is ~250 nm, and depends on the wavelength of the light that builds the image (Chapter 2) and the NA of the lens (Figure 3.31). Resolution along the optical axis is proportional to NA^{-2}. With NA being greater than 1 for good lenses, it is worse than ~700 nm. The size of most subcellular structures is well below the resolution limit. For example, the thickness of biological membranes is 5–10 nm, the diameter of an actin filament is about 7 nm, the diameter of a microtubule is about 25 nm, and early endosomes can have a diameter of 100 nm. This means that a typical optical microscope cannot resolve folds of the inner mitochondrial membrane, closely spaced actin fibers, microtubules, or endosomes. Such structures are readily resolved by an electron microscope. However, live-cell studies cannot be performed with this technique owing to too large a thickness of intact cells and the damage induced by the beam of electrons. Thus, for the biologist there is a need for a substantially better spatial resolution to be achieved by fluorescence microscopy. This goal has now been attained by several new microscopy techniques. They are introduced in Chapters 8–10.

3.7.5 Misrepresentation of Small Objects

Even the smallest light-emitting object, such as a molecule of eGFP, will be represented on a fluorescence microscopy image by a diffraction-limited signal, which is a bright circle of a diameter not smaller than ~250 nm in the plane of the

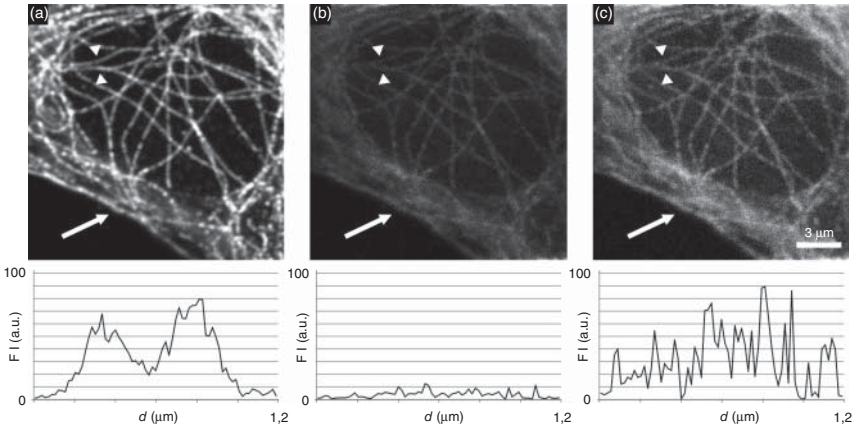

Figure 3.30 The influence of signal-to-noise ratio (S/N) on image quality. (a) An image of microtubules stained by immunofluorescence was recorded at a high fluorescence signal-to-noise ratio. Arrowheads point at the line along which the fluorescence profile (below), running across two microtubules, was drawn. (b) The same area imaged when the S/N ratio was made low due to photobleaching. (c) The image shown in (b) after increasing the brightness. The fluorescence profiles in panels (a), (b), and (c) demonstrate that image resolution becomes significantly lower when the S/N decreases. The two microtubules become visually unresolvable when the intensity of fluorescence signal is low in comparison to the noise. A loss of image resolution can also be seen clearly in the area marked with an arrow. (Images courtesy of Agnieszka Pierzyńska-Mach, Jagiellonian University, Kraków.)

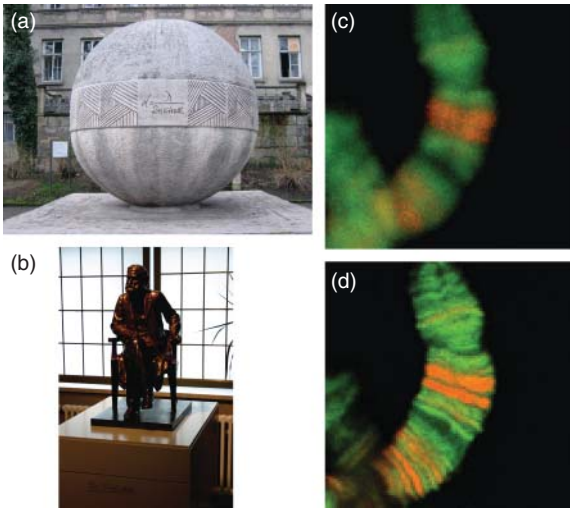

Figure 3.31 The Abbe formula and the role of numerical aperture in image resolution. (a) Abbe's formula engraved on a monument in Jena and (b) a statue of Ernst Abbe in the Optisches Museum of Jena. (c,d) Images showing a fragment of a polytene chromosome from *Chironomus tentans*, stained for condensed and relaxed chromatin. The images were recorded using a (c) 0.7 and (d) 1.4 NA lens, respectively, and demonstrate the substantially higher resolution at higher NA. The original image (d) is much brighter than image (c) owing to the higher NA; therefore, the brightness of (c) was increased for clarity. (Images by W. Krzeszowiec and J. Dobrucki, Jagiellonian University, Kraków.)

specimen. This means that the size of objects smaller than ~250 nm will be misrepresented by a fluorescence microscope (Figure 3.32). Paradoxically, this means that an observer has to interpret fluorescence images carefully. The size of the cell and the nucleus are represented correctly, but the diameter of actin fibers, microtubules, early endosomes, and the thickness of the plasma membrane, all seen in the same image, will be seriously exaggerated and appear much larger and out of scale in comparison with the cell size.

3.8 Summary and Outlook

Fluorescence microscopy has witnessed an unprecedented growth in the past 20 years. Successful efforts to develop this area of technology have followed several avenues of research. These include studies of dynamic events using FRAP, FRET, speckle microscopy, fluorescence correlation spectroscopy (FCS), and FLIM techniques (Chapters 5, 11, and 13). New trends also include high-resolution stimulated emission depletion (STED) microscopy, structured illumination (SI) microscopy, PALM, and STORM, as well as high-sensitivity and large-area-of-view light sheet fluorescence microscopy [21] (Chapters 5, 6, 8–10) and a microscope equipped with a mesolens. Modern optical microscopy instrumentation has also been developed to study large numbers of cells (laser

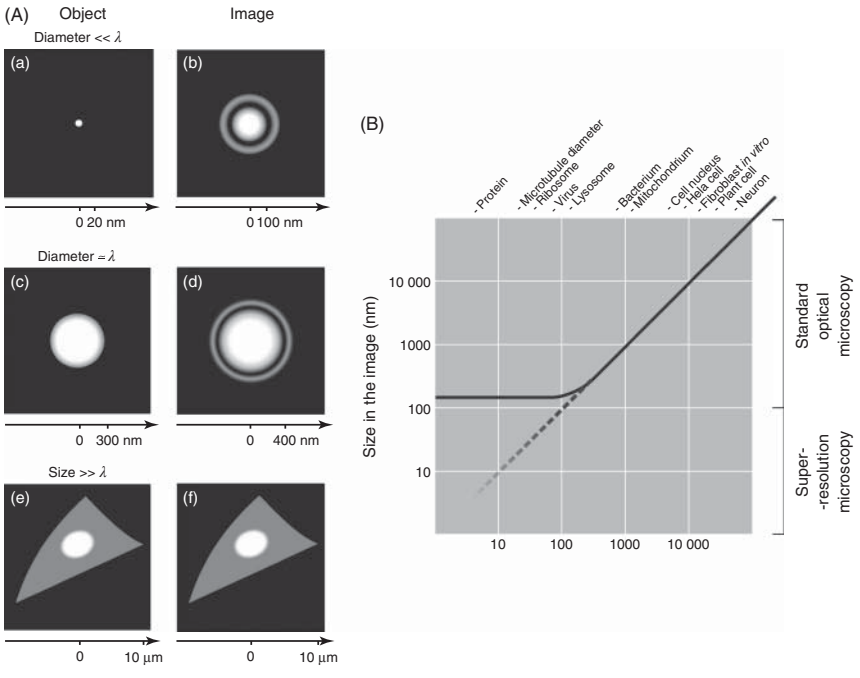

Figure 3.32 Misrepresentation of small objects in fluorescence microscopy. (A) A schematic representation of small objects (left) and their images (right) generated by a standard fluorescence microscope. An image of a bright 3 nm diameter sphere (shown in (a)) is a large circle ~250 nm in diameter, surrounded by interference fringes (b). When a sphere with a diameter comparable to the wavelength of light (a few hundred nanometers) (c) is imaged, the diameter of the image reflects the real size reasonably well (d), that is, in a correct proportion to the field of view; interference effects appear at the edges. When animal cells *in vitro* with a size of 10–30 µm (e) are imaged, their size and shape are reflected correctly and interference effects are less noticeable (f). Note that the object in (a) and the corresponding image (b) are not drawn to scale. If proportions between a 3 nm sphere and the corresponding image were to be maintained, the image (b) would have to be larger than the page on which it is printed. The intensity of interference fringes is exaggerated in diagrams (b) and (d). (B) Relationship between the true size of the object and the size of this object in a fluorescence microscopy image. The smaller the object, the greater (relatively) the distortion. The relative contribution of interference fringes is also greater in images of small objects. Cell components such as protein molecules (if detectable at all) or the thickness of the plasma membrane will appear too large in relation to bigger objects such as the nucleus, and to the whole cell in the same image. New super-resolution microscopy methods are aiming at increasing the spatial resolution and reducing the misrepresentation of small objects. (Adapted from Dobrucki [10], with kind permission of Elsevier.)

scanning cytometry (LSC), high-throughput screening, "image-in-stream" – an extension of flow cytometry). The expansion of these techniques has been facilitated by the development of new low molecular weight and fluorescent protein probes and labels (Chapter 4) and new image analysis tools. Thus, fluorescence microscopy has developed into an analytical tool capable of performing biochemical studies in intact living cells.

References

1 Herschel, J.F.W. (1845) No. I. On a case of superficial colour presented by a homogeneous liquid internally colourless. *Philos. Trans. R. Soc. London*, **135**, 143–145.

2 Herschel, J.F.W. (1845) No. II. On the epipolic dispersion of light, being a supplement to a paper entitled, "On a case of superficial colour presented by a homogeneous liquid internally colourless". *Philos. Trans. R. Soc. London*, **135**, 147–153.

3 Stokes, G.G. (1852) On the change of refrangibility of light. *Philos. Trans. R. Soc. London*, **142**, 463–562.

4 Jabłoński, A. (1945) General theory of pressure broadening of spectral lines. *Phys. Rev.*, **68** (3-4), 78–93.

5 Brown, R.H. and Twiss, R.Q. (1957) Interferometry of the intensity fluctuations in light. I. Basic theory: the correlation between photons in coherent beams of radiation. *Proc. R. Soc. London, Ser. A*, **242** (1230), 300–324.

6 Axelrod, D., Ravdin, P., Koppel, D.E., Schlessinger, J., Webb, W.W., Elson, E.L., and Podleski, T.R. (1976) Lateral motion of fluorescently labeled acetylcholine receptors in membranes of developing muscle fibers. *Proc. Natl. Acad. Sci. U.S.A.*, **73** (12), 4594–4598.

7 Knight, M.M., Roberts, S.R., Lee, D.A., and Bader, D.L. (2003) Live cell imaging using confocal microscopy induces intracellular calcium transients and cell death. *Am. J. Physiol. Cell Physiol.*, **284** (4), C1083–C1089.

8 Bernas, T., Zarębski, M., Cook, P.R., and Dobrucki, J.W. (2004) Minimizing photobleaching during confocal microscopy of fluorescent probes bound to chromatin: role of anoxia and photon flux. *J. Microsc.*, **215** (3), 281–296 (Erratum in: *J. Microsc.* (2004) **216** (Pt 2), 197).

9 Diaspro, A., Chirico, G., Usai, C., Ramoino, P., and Dobrucki, J. (2006) in *Handbook of Biological Confocal Microscopy*, 3rd edn (ed. J. Pawley), Springer, New York, pp. 690–702.

10 Dobrucki, J.W. (2004) Confocal microscopy: quantitative analytical capabilities. *Methods Cell Biol.*, **75**, 41–72.

11 Tsien, R.Y., Ernst, L., and Waggoner, A. (2006) in *Handbook of Biological Confocal Microscopy*, 3rd edn (ed. J. Pawley), Springer, New York, pp. 338–352.

12 Rajwa, B., Bernas, T., Acker, H., Dobrucki, J., and Robinson, J.P. (2007) Single- and two-photon spectral imaging of intrinsic fluorescence of transformed human hepatocytes. *Microsc. Res. Tech.*, **70** (10), 869–879.

13 Dobrucki, J.W., Feret, D., and Noatynska, A. (2007) Scattering of exciting light by live cells in fluorescence confocal imaging: phototoxic effects and relevance for FRAP studies. *Biophys. J.*, **93** (5), 1778–1786.

14 Betzig, E., Patterson, G.H., Sougrat, R., Lindwasser, O.W., Olenych, S., Bonifacino, J.S., Davidson, M.W., Lippincott-Schwartz, J., and Hess, H.F. (2006) Imaging intracellular fluorescent proteins at nanometer resolution. *Science*, **313** (5793), 1642–1645.

15 van de Linde, S., Löschberger, A., Klein, T., Heidbreder, M., Wolter, S., Heilemann, M., and Sauer, M. (2011) Direct stochastic optical reconstruction microscopy with standard fluorescent probes. *Nat. Protoc.*, **6** (7), 991–1009.
16 Rust, M.J., Bates, M., and Zhuang, X. (2006) Sub-diffraction-limit imaging by stochastic optical reconstruction microscopy (STORM). *Nat. Methods*, **3** (10), 793–795.
17 Sinnecker, D., Voigt, P., Hellwig, N., and Schaefer, M. (2005) Reversible photobleaching of enhanced green fluorescent proteins. *Biochemistry*, **44** (18), 7085–7094.
18 Baddeley, D., Jayasinghe, I.D., Cremer, C., Cannell, M.B., and Soeller, C. (2009) Light-induced dark states of organic fluorochromes enable 30 nm resolution imaging in standard media. *Biophys. J.*, **96** (2), L22–L24.
19 Żurek-Biesiada, D., Kędracka-Krok, S., and Dobrucki, J.W. (2013) UV-activated conversion of Hoechst 33258, DAPI, and Vybrant DyeCycle fluorescent dyes into blue-excited, green-emitting protonated forms. *Cytometry Part A*, **83** (5), 441–451.
20 Klein, T., van de Linde, S., and Sauer, M. (2012) Live-cell super-resolution imaging goes multicolor. *ChemBioChem*, **13** (13), 1861–1863.
21 Verveer, P.J., Swoger, J., Pampaloni, F., Greger, K., Marcello, M., and Stelzer, E.H. (2007) High-resolution three-dimensional imaging of large specimens with light sheet-based microscopy. *Nat. Methods*, **4** (4), 311–313.
22 Zhao, H., Dobrucki, J., Rybak, P., Traganos, F., Halicka, D., and Darzynkiewicz, Z. (2011) Induction of DNA damage signaling by oxidative stress in relation to DNA replication as detected using "click chemistry". *Cytometry A.*, **79** (11), 897–902.
23 Biela, E., Galas, J., Lee, B., Johnson, G., Darzynkiewicz, Z., and Dobrucki, J.W. (2013) Col-F, a fluorescent probe for ex vivo confocal imaging of collagen and elastin in animal tissues. *Cytometry A.*, **83** (6), 533–539.
24 Berniak, K., Rybak, P., Bernaś, T., Zarębski, M., Biela, E., Zhao, H., Darzynkiewicz, Z., and Dobrucki, J.W. (2013) Relationship between DNA Damage Response, initiated by camptothecin or oxidative stress, and DNA replication, analyzed by quantitative image analysis. *Cytometry A.*, **83** (10), 913–924.
25 Zarębski, M., Kordon, M., and Dobrucki, J.W. (2014) Photosensitized damage inflicted on plasma membranes of live cells by an extracellular generator of singlet oxygen–a linear dependence of a lethal dose on light intensity. *Photochem Photobiol.*, **90** (3), 709–15.

Recommended Internet Resources

http://micro.magnet.fsu.edu/primer/ by Michael W. Davidson and The Florida State University.
http://www.nobelprize.org/nobel_prizes/medicine/laureates/1906/golgi-lecture.html.
http://www.nobelprize.org/nobel_prizes/medicine/laureates/1906/press.html.
http://www.nobelprize.org/nobel_prizes/physics/laureates/1953/press.html.

http://www.nobelprize.org/nobel_prizes/physics/laureates/1953/zernike-lecture.html.
http://www.nobelprize.org/nobel_prizes/chemistry/laureates/2008/shimomura-lecture.html.
http://www.nobelprize.org/search/?query=chalfie.
http://www.nobelprize.org/search/?query=tsien.
http://www.univie.ac.at/mikroskopie/
http://www.nobelprize.org/nobel_prizes/chemistry/laureates/2014/advanced.html.
http://www.andor.com/learning-academy/ccd-spectral-response-%28qe%29-defining-the-qe-of-a-ccd.

Fluorescent Spectra Database

http://www.spectra.arizona.edu/.